Stratosphere-to-troposphere transport: A model and method evaluation

P. Cristofanelli,[1] P. Bonasoni,[1] W. Collins,[2] J. Feichter,[3] C. Forster,[4] P. James,[4] A. Kentarchos,[5] P. W. Kubik,[6] C. Land,[3] J. Meloen,[7] G. J. Roelofs,[5] P. Siegmund,[7] M. Sprenger,[8] C. Schnabel,[9,10] A. Stohl,[4] L. Tobler,[11] L. Tositti,[12] T. Trickl,[13] and P. Zanis[14]

Received 31 May 2002; revised 25 September 2002; accepted 1 October 2002; published 13 March 2003.

[1] During the EU-project Influence of Stratosphere-Troposphere exchange in a Changing Climate on Atmospheric Transport and Oxidation Capacity (STACCATO), a combined approach of a measurement network and numerical simulations was used to estimate the strength and frequency of stratosphere-to-troposphere transport (STT) events and their influence on tropospheric chemistry. Measurements of surface ozone, beryllium-7, and beryllium-10 concentrations and meteorological parameters at four European high mountain stations, as well as atmospheric profiles obtained by ozone soundings and a high-resolution lidar, were carried out. In order to simulate STT events, seven different models have been applied by the STACCATO partners. These are two trajectory models (LAGRANTO and FLEXTRA), a Lagrangian transport model (FLEXPART), a Lagrangian chemistry-transport model (STOCHEM), a Eulerian transport model (TM3), and two general circulation models (ECHAM4 and MA-ECHAM4). In order to investigate the strengths and weaknesses of each of these models and to identify the reasons for their discrepancies, a detailed comparison with measured data is presented in this paper. These models provided fluxes and concentrations of a stratospheric tracer, as well as the vertical profiles of ozone and radionuclides for a stratospheric intrusion case study that occurred over Europe in the year 1996. The comparison of the model results with the measurement data and the satellite observations revealed that all the models captured the general behavior of the event. However, great differences were found in the intensity and spatial development of the simulated intrusion event. *INDEX TERMS:* 0368 Atmospheric Composition and Structure: Troposphere—constituent transport and chemistry; 3337 Meteorology and Atmospheric Dynamics: Numerical modeling and data assimilation; 3362 Meteorology and Atmospheric Dynamics: Stratosphere/troposphere interactions; *KEYWORDS:* stratosphere-to-troposphere exchange, stratospheric intrusion, model validation, stratospheric tracers

Citation: Cristofanelli, P., et al., Stratosphere-to-troposphere transport: A model and method evaluation, *J. Geophys. Res.*, *108*(D12), 8525, doi:10.1029/2002JD002600, 2003.

1. Introduction

[2] Stratosphere-troposphere exchange (STE) is one of the most important factors controlling the levels of ozone, water vapor and other compounds both in the stratosphere and in the upper troposphere. According to the nomenclature defined by A. Stohl et al. (Stratosphere-troposphere exchange: A review and what we have learned from STACCATO, submitted to *Journal of Geophysical Research*, 2003), the expression stratosphere-to-troposphere transport

[1]National Research Council, Institute of Atmosphere Sciences and Climate, Bologna, Italy.
[2]Climate Research, Met Office, Bracknell, UK.
[3]Max-Planck Institute for Meteorology, Hamburg, Germany.
[4]Department of Ecology, Technical University of Munich, Freising-Weihenstephan, Germany.
[5]Institute for Marine and Atmospheric Research, University of Utrecht, Utrecht, Netherlands.
[6]Paul Scherrer Institute, Zurich, Switzerland.
[7]Division of Atmospheric Composition, Royal Netherlands Meteorological Institute, de Bilt, Netherlands.
[8]Institute for Atmospheric and Climate Sciences, Swiss Federal Institute of Technology Zurich, Zurich, Switzerland.
[9]Deparment of Chemistry and Biochemistry, University of Berne, Berne, Switzerland.
[10]Institute of Particle Physics, Eidgenossische Technische Hochschule Hoenggerberg, Zurich, Switzerland.
[11]Paul Scherrer Institute, Villigen, Switzerland.
[12]Environmental Radiochemistry Laboratory, Bologna University, Bologna, Italy.
[13]Institut fuer Meteorologie und Klimaforschung, Bereich Atmosphaerische Umweltforschung, Forschungzentrum Karlsruhe, Garmisch-Partenkirchen, Germany.
[14]Laboratory of Atmospheric Physics, Aristotle University of Thessaloniki, Greece.

0148-0227/03/2002JD002600$09.00

(STT) is used in this paper to refer specifically to stratospheric intrusion phenomena. The most important phenomena promoting STT events are associated with tropopause folds and cut-off lows. Tropopause folds are related to rapid surface cyclogenesis [*Reed*, 1955] or strong frontal activity with the development of jet stream instability in the middle-upper troposphere or in the lower stratosphere [*Danielsen*, 1968; *Buzzi et al.*, 1984]. During these events, a frontogenically induced ageostrophic circulation can bring stratospheric air to reach lower altitudes and troposphere. Turbulence near the jet and diabatic erosion of the tropopause can then lead to irreversible mixing of stratospheric and tropospheric air. In a cut-off low, STT can be caused by convective erosion of the tropopause and turbulent mixing inside the cyclonic vortex or by tropopause folding during the vortex formation or its intensification [*Vaughan and Price*, 1989]. Although the tropopause folds related to cut-off lows are less intense than those associated with jet stream instability, they are considered to be more frequent [*Price and Vaughan*, 1992].

[3] From a statistical analysis concerning deep stratospheric intrusion events at two mountain stations in the Alpine area (Zugspitze and Wank) during a 10-year measurement period, *Elbern et al.* [1997] concluded that the lower troposphere was significantly influenced by stratospheric air masses during 5% of all days and the annual average of the monthly enrichment rate of ozone (O_3) concentration was about 3%. However, the statistical analysis of stratospheric intrusions based on experimental data is strongly dependent on the criteria used to select the events [*Scheel et al.*, 1999]. In fact, by a different methodology *James et al.* [2003] estimated that about 9% of the fraction of O_3 was due to pronounced STTs in the period 1990–1999 at the Zugspitze. A climatology of stratospheric O_3 transported to high-Alpine sites during STT events based on both model results and measurement data [*Stohl et al.*, 2000], showed that during the late winter/early spring direct STT events (i.e., those that occurred close to the measurement stations and left a clear signal in the measurement data) contributed about 15–25% to the recorded O_3. In a previous study *Austin and Follows* [1991] and *Follows and Austin* [1992], suggested that 25% of the O_3 at 300 hPa has a stratospheric origin, while at 700 hPa this influence decreased to 10% and at surface level to 5%. Using a coupled general circulation-chemistry model *Roelofs and Lelieveld* [1997] found that 40% of the tropospheric O_3 originated in the stratosphere. There are evident discrepancies between the different experimental and modeling studies which can be attributed to many factors. In the experimental studies the detection of STT events is strictly related to the altitude of the measurement site, its geographical location as well as the number, the types and the sampling time resolution of atmospheric tracers monitored. In fact, after crossing the tropopause, stratospheric air starts to mix with tropospheric air, losing part of its original properties. Moreover, STT events often have a very short duration that cannot be captured by measurements with a too coarse time resolution.

[4] In order to reduce these uncertainties, different models are used to diagnose STT events by the partners of the EU project Influence of Stratosphere-Troposphere Exchange in a Changing Climate on Atmospheric Transport and Oxidation Capacity (STACCATO). The seven models are shortly characterized in Table 1. There are two trajectory models (LAGRANTO and FLEXTRA), a Lagrangian particle dispersion model (FLEXPART), a Lagrangian chemistry model coupled to a climate model (STOCHEM), a Eulerian chemistry model (TM3), a general circulation model (MA-ECHAM4) and a chemistry-general circulation model (ECHAM4). The general circulation models (GCMs) were nudged toward ECWMF analyses for the period considered (for more details on the models see *Meloen et al.* [2003]). Besides using different input data, the models are characterized by different horizontal, vertical and temporal resolution. Some, but not all, included convection and PBL schemes. These models, widely used in STACCATO to establish global climatologies of STE and its influence on the tropospheric O_3 budget, are usually used for quite different purposes and focus on very different aspects of STE (e.g., air chemistry studies, transport climatologies). However, it was considered important to bring them all together for a joint study and to compare them with each other. Thus, they have been applied to study in detail one STT event for which an excellent set of measurement data was available. An intercomparison between the different models is presented in a companion paper by *Meloen et al.* [2003] while in this work we compare the models with available measurement data. The extended measurement network that was used within the STACCATO project (Figure 1) consisted of four mountain stations (Jungfraujoch: JUN; Sonnblick: SON; Zugspitze: ZUG; Mt. Cimone: CIM), a high-resolution ozone lidar (Garmisch Partenkirchen: GAR) and an ozone sounding station (S. Pietro Capofiume: CAP). The area covered by the STACCATO measurement sites is known to be frequently subjected to STT [*Davies and Schuepbach*, 1994]. In fact, lee cyclogenesis is quite frequent in the Alpine region [*Buzzi et al.*, 1984; *Buzzi et al.*, 1985; *Tafferner*, 1990; *Aebischer and Schaer*, 1998] and leads to frequent STT episodes [*Schuepbach et al.*, 1999]. At CIM *Bonasoni et al.* [2000] identified 26 events of high ozone levels associated with transport from the lower stratosphere/upper troposphere within a 2-year period, while over GAR lidar measurements could be carried out during 42 stratospheric intrusion episodes in 1996 and 1997 [*Eisele et al.*, 1999].

[5] This paper is structured as follows: the measurement data and the model products used to investigate the STT event are briefly described in the next section. Section 3 presents the results of the comparison, which are discussed in section 4, where the conclusions are drawn.

2. Stratospheric Tracers: Experimental and Modeling Approach

[6] The different data obtained at the STACCATO stations are summarized in Table 2. Vertical sounding by a high-resolution O_3 lidar at GAR and by ozone-soundings (O_3, relative humidity and specific humidity) at CAP and at two stations not directly involved in the STACCATO project (Payerne: PAY; Hohenpeißenberg: HOH), were utilized. Furthermore, we used continuous measurements of relative humidity (RH), O_3, beryllium-7 (Be-7) and beryllium-10 (Be-10) concentrations carried out at the four high mountain stations JUN, CIM, SON and ZUG. These

Table 1. Overview of the Methods and Models Evaluated[a]

Model	LAGRANTO	FLEXTRA	FLEXPART	STOCHEM	TM3	ECHAM4	MA-ECHAM4
Institute	ETHZ	TUM	TUM	MetO	KNMI	IMAU	MPI
Type of model	Trajectory	Trajectory	Lagrangian	Lagrangian transport	Eulerian transport	Nudged GCM	Nudged GCM
Reference	*Wernli and Davies* [1997]; *Stohl et al.* [2001]	*Stohl et al.* [1995]; *Stohl et al.* [2001]	*Stohl et al.* [1998]; *Stohl and Thomson* [1999]	*Collins et al.* [1997, 2003]	*Meijer et al.* [2000]	*Roeckner et al.* [1996]; *Jeuken et al.* [1996]	*Manzini and McFarlane* [1998]; *Jeuken et al.* [1996]
Input data	First guess ECWMF data						
Horizontal resolution	1° × 1°	1° × 1°	1° × 1°	3.75° × 2.5°	2.5° × 2.5°	1.85° × 1.85°	3.75° × 3.75°
Vertical resolution (no. of levels)	31	31	31	38	31	19	39 (top 0.01 hPa)
Temporal resolution input data	6 hours	3 hours	3 hours	6 hours	6 hours	6 hours	6 hours
Convection scheme	No	No	Yes	Yes	Yes	Yes	Yes
PBL scheme	No	No	Yes	Yes	Yes	Yes	Yes

[a]From *Meloen et al.* [2003].

parameters are the principal tracers used to identify STTs. In fact, stratospheric air is characterized by high O_3 concentrations and low RH. However, due to the dilution and mixing with tropospheric air, STT events at mountain stations are not always associated with clearly elevated O_3 and low RH conditions. Furthermore, low RH values are also characteristic for air that has descended from the upper troposphere and was warmed adiabatically. High concentrations of the cosmogenic radionuclide Be-7 ($t_{1/2}$ = 53.2 days) are also indicative for STTs [*Reiter et al.*, 1983], but Be-7 can be removed by wet scavenging of the carrier aerosol. In addition, because one third of Be-7 is produced in the upper troposphere [*Koch and Mann*, 1996; *Koch et al.*, 1996; *Dutkiewicz and Husain*, 1985], it is an ambiguous stratospheric tracer [*Zanis et al.*, 1999; *Stohl et al.*, 2000]. Therefore, during STACCATO, measurements of Be-10 concentrations were performed using the same air filters as for Be-7 determination. Be-10 is formed by nuclear

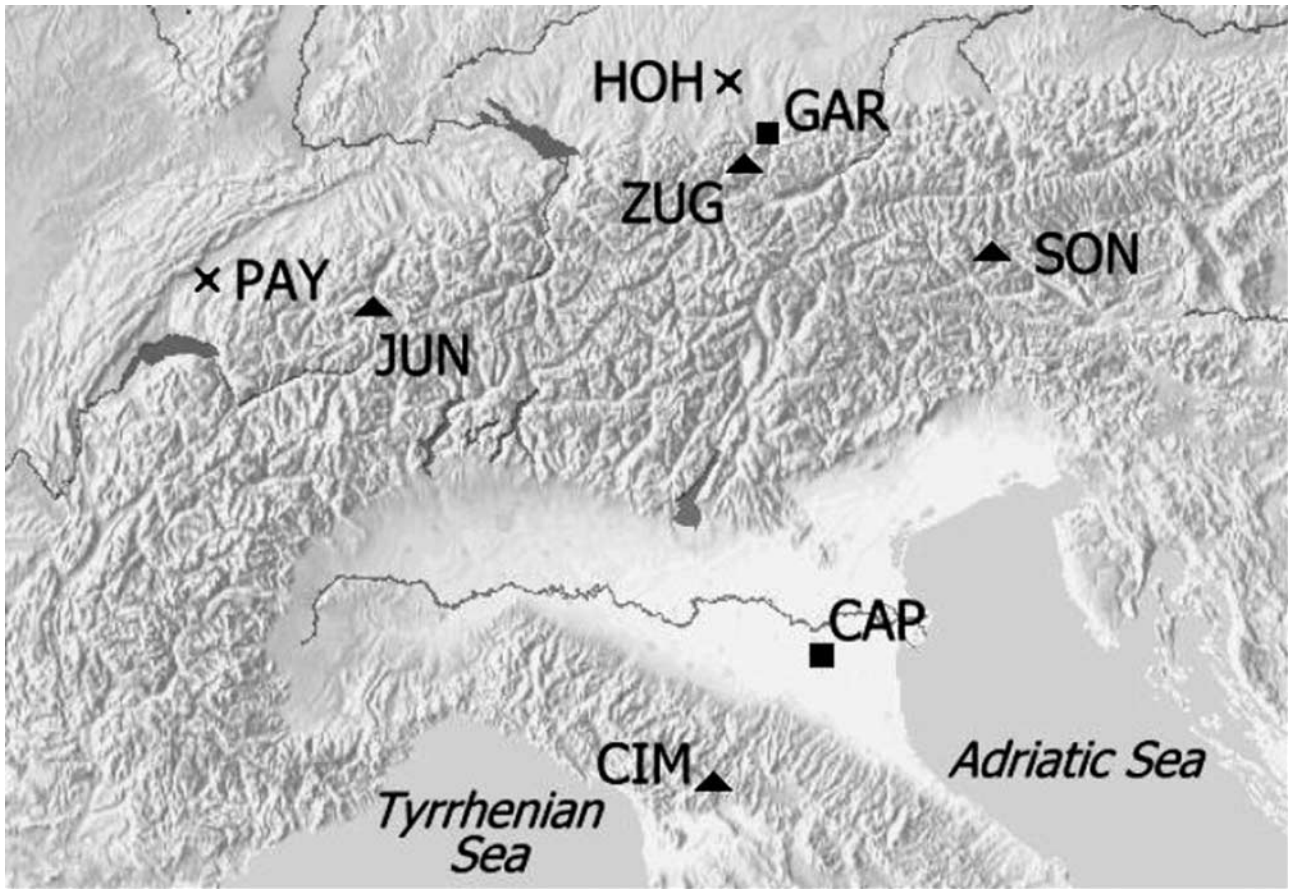

Figure 1. Geographical location of the STACCATO measurement stations. Triangles represent the mountain stations, squares the atmospheric sounding stations and crosses the extra-STACCATO stations.

Table 2. Overview of Data Availability at the STACCATO Stations During the Case Study (26 May to 7 June 1996)

Type of Station	Station	Location	Type of Measurement	Data Availability During Case Study
Mountain Station	JUN	46.5N; 8.0E; 3576 m asl	Ozone	86%
			Relative humidity	100%
			Radionuclides	Be-7: 100%; Be-10: 100% Sampling time: 48 hours
	CIM	44.2N; 10.7E; 2165 m asl	Ozone	100%
			Relative humidity	100%
			Radionuclides	Be-7: 30–31/05; Be-10: No data; Sampling time 24 hours
	SON	47.0N;12.9E; 3106 m asl	Ozone	100%
			Relative humidity	68 %
			Radionuclides	Be-7 and Be-10: No data
	ZUG	47.4N; 11.0E 2962 m asl	Ozone	100%
			Relative humidity	100%
			Radionuclides	Be-7: 100%; Be-10: No data; Sampling time 24 hours
Vertical Sounding Station	GAR	47.5N; 11.5E; 74 m asl	LIDAR profile	From 29 May to 7 June; Missing data: 2–4 June
	HOH	47.8N; 11.0E; 985 m asl	Ozone-sounding	29 May; 31 May; 3 June; 5 June (at 0600 UTC)
	PAY	46.8N; 6.9E; 501 m asl	Ozone-sounding	28 May; 29 May; 31 May; 03 June; 06 June (at 1200 UTC)
	SPC	44.6N; 10.6N; 10 m asl	Ozone-sounding	03 June (at 1200 UTC)

spallation reactions in the stratosphere and upper troposphere. Due to its long half-life ($t_{1/2} = 1.5 \times 10^6$ years) "it has essentially zero decay probability in the atmosphere" [*Raisbeck et al.*, 1981], but it is removed by wet deposition in the same way as Be-7. Thus, the ratio Be-10/Be-7 should be a very sensitive parameter to identify STTs, as it is higher in the stratosphere than in the troposphere [*Raisbeck et al.*, 1981; *Dibb et al.*, 1994].

[7] STT events are also seen as regions of dry air in water vapor (WV) images from meteorological satellites. The observations within the Meteosat 6-μm WV channel are very sensitive to dry air in the upper troposphere [*Appenzeller and Davies*, 1992; *Appenzeller et al.*, 1996; *Wirth et al.*, 1997] and can be useful to describe the spatial extensions of the dry air stream from the stratosphere. The instrument is most sensitive at around 450 hPa for very dry conditions in the upper troposphere, while for a moist upper troposphere the highest sensitivity is at higher levels [*Fischer et al.*, 1982].

[8] In order to simulate the stratospheric intrusion event, each model group was asked to calculate the transport of an idealized *stratospheric tracer* that was characterized by a mixing ratio kept constant at 1 kg/kg in the stratosphere (above the tropopause level defined as the 2 pvu potential vorticity surface, where 1 pvu = 10^{-6} K m^2 kg^{-1} s^{-1}) and by a decay time of 2 days in the troposphere (more detail on the models setup [*Meloen et al.*, 2003]). The main purpose of this tracer was to compare how the different models simulate its transport. Having a decay time of only 2 days, this tracer is also a good indicator where stratospheric air has recently intruded into the troposphere. Its spatial distribution should, thus, agree at least qualitatively with the measurements of the various stratospheric tracers at the measurements stations. In addition, some models also explicitly calculated the vertical profiles of O_3, Be-7 and Be-10 over the measurement sites (see Table 3).

3. Case Study: Episode From 26 May to 7 June 1996

3.1. Case Study: Synoptic and Meteorological Description

[9] The studied STT episode occurred during the period 26 May 1996 to 7 June 1996. It was already extensively studied during the projects VOTALP and VOTALP II and thus we provide here only a brief description of the respective synoptic situation (for more detailed descriptions see *Feldmann et al.* [1999], *Eisele et al.* [1999], *Bonasoni et al.* [2000], and *Stohl et al.* [2000]). During this period, two STT events influenced great parts of central and southern Europe and were recorded at the mountain and sounding stations. On 28 May, a streamer with stratospheric PV values extended from Scandinavia to the Alpine region on the 310 K isentropic surface [*Stohl et al.*, 2000]. This streamer is seen as a band of dry air extending from Scandinavia to southern Italy in the Meteosat WV image (Figure 2a). Since 29 May, anticyclonic subsidence was present in the western part of the fold, where the stratospheric air was transported downward into the middle troposphere over the Alps and the northern Apennines. On the same day a low was cut off in the Mediterranean.

[10] The second STT event developed on 2 June 1996 when the 500 hPa chart showed a trough from Scotland to Algeria together with stratospheric values of PV on the 310 K isentropic surface. A cyclonic vortex, visible in the WV map (Figure 2b), developed over the Gulf of Genoa and was cut off on 4 June 1996.

3.2. Stratospheric Tracer Flux Over the Model Domain

[11] In order to evaluate the capability of the different tools of describing the stratospheric intrusion at high tropospheric levels, the Meteosat WV image is compared with the spatial distribution of the stratospheric tracer as calculated by models. Ideally, the comparison should be made with vertical columns of the stratospheric tracer, but as this was not available from all the models, we compare the maps of the net stratospheric tracer flux at 500 hPa. It must be kept in mind that the dark regions in the WV Meteosat images are not always indicative of stratospheric air, but can also be associated with air descending only from the upper troposphere.

[12] Generally, the streamer of dry air seen in the satellite observations was captured by all the models (Figure 3). In fact, for LAGRANTO, FLEXTRA and FLEXPART a narrow band of high downward stratospheric tracer flux (greater than 10^{-2} kg m^{-2} s^{-1}) overlapped very well with the Meteosat dry air stream. For TM3, ECHAM4 and MA-ECHAM4, the geographical domain was almost entirely filled by traces of the stratospheric tracer. In fact, the two GCM models simulated high values of downward strato-

Table 3. Overview of Parameters Calculated by Models and Used in the Evaluation Exercise[a]

Model	LAGRANTO	FLEXTRA	FLEXPART	STOCHEM	TM3	ECHAM4	MA-ECHAM4
[ST] vertical profile	yes	yes	yes	yes	yes	yes	yes
[SH] vertical profile	yes	yes	yes	no	no	yes	yes
[O_3] vertical profile	no	no	no	yes	no	yes	no
[Be-7] and [Be-10] vertical profile	no	no	no	yes	no	no	yes
ST flux over model domain	yes	yes	yes	yes	yes	yes	yes

[a]Brackets indicate simulated concentrations.

spheric tracer flux, covering a region largely exceeding the narrow dry air stream. As reported by *Meloen et al.* [2003], this effect is related both to the relatively coarse resolution of the models and to the numerical diffusion that affects especially the ECHAM4 and MA-ECHAM4 results. On the other hand, the TM3 results show only rather small values outside the Meteosat dry streamer, because TM3 uses an advection scheme less diffusive than the two GCMs. Moreover, in contrast to TM3, ECHAM4 and MA-ECHAM4 advect the tracer on-line, thus the fluctuations in the wind field possibly can transport larger amounts of the stratospheric tracer into the troposphere. The effect of the higher horizontal resolution of ECHAM4 is emphasized by the differences between the results of the two GCMs. STOCHEM only roughly identified the pattern of the dry air mass, probably due to its coarse resolution and its too small number of air parcels used [*Meloen et al.*, 2003].

3.3. Stratospheric Tracer Concentrations

[13] Next, we evaluate the time series of the stratospheric tracer concentrations([ST]) calculated for the mountain stations. We compared [ST], averaged between 600 and 800 hPa, with the O_3, RH, Be-7 and Be-10 recorded during the event. We considered 600–800 hPa because this is the range that includes the altitudes of all the mountain stations considered. This vertical averaging also minimizes problems related to the differences between the real topography and the model topographies, which can be quite large. Due to the specific nature of the stratospheric tracer calculated by models, only a ''qualitative'' comparison with the measurements data was possible. For those models that

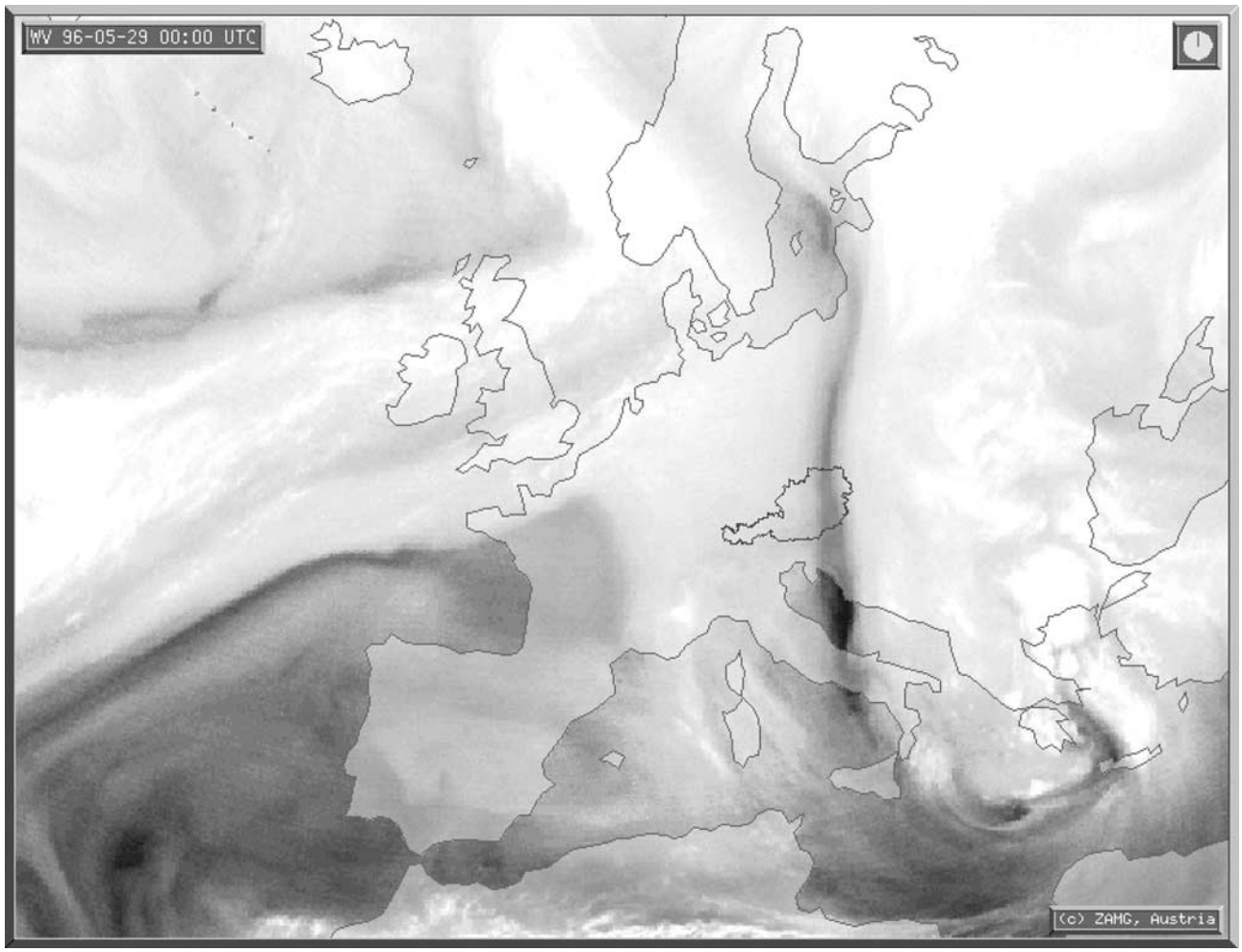

Figure 2. Water vapor Meteosat image on 29 May 1996 at 1000 UTC (plate A) and on 3 June 1996 at 1800 UTC (plate B).

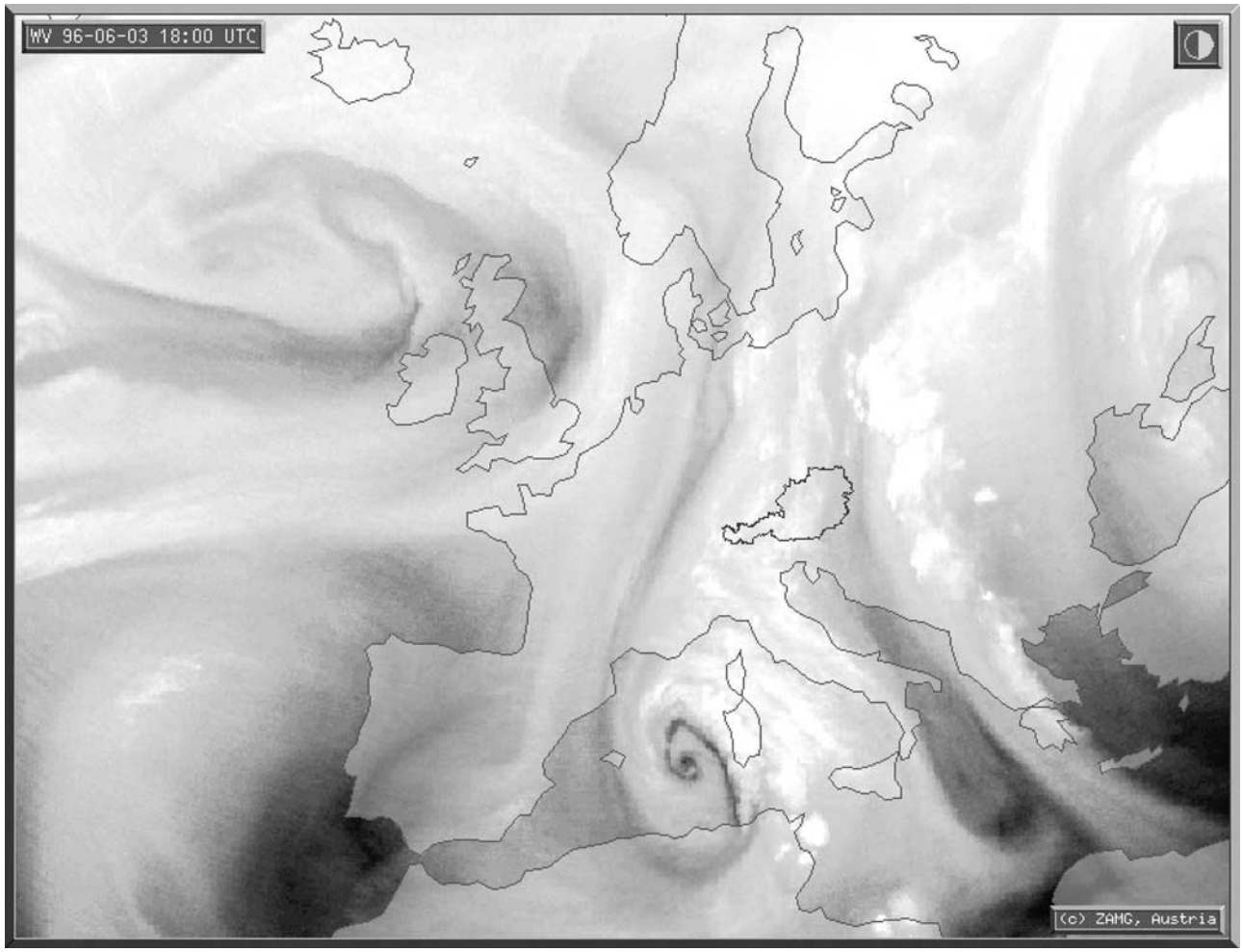

Figure 2. (continued)

provided measurable parameters (i.e. O_3, Be-7, Be-10), they were compared also quantitatively to the measurements. In this section, each paragraph presents the results of each model for the mountain stations. Particularly, we focus on the strongest STT evidences recorded at JUN, where Be-10 measurements were available, and CIM, the only summit station south of the Alps.

[14] At JUN, the arrival of stratospheric air was evidenced by a maximum in O_3 and Be-7 (77 ppb and 11 mBq/m^3 respectively) as well as by a decrease in the RH starting on 28 May at 1900 UTC (hour 67 since 26 May 1996 at 0000 UTC in Figure 4). During the second STT event, high values of O_3 (68 ppb) and Be-7 (10 mBq/m^3) together with a drop in RH (31%) were recorded around hour 252. In the northern Apennines, as recorded at CIM, the strongest experimental evidences of the STT event occurred between hour 108 and 132, when ozone hourly concentrations increased to 90 ppb, RH dropped to 0% and Be-7 reached 15 mBq/m^3.

3.3.1. LAGRANTO and FLEXTRA

[15] For JUN, LAGRANTO and FLEXTRA showed similar results, characterized by sporadic spikes in [ST] (Figure 4). The time versus height analysis showed a clear tropopause lowering between hour 24 and 48 (Figure 5). However, the low SH stream simulated below 700 hPa around hour 60, was not completely related to high [ST] values. At CIM, LAGRANTO and FLEXTRA (Figure 6) showed continuous high [ST] values (exceeding 10^{-1} kg/kg) between hours 120 and 135. The models represented the intrusion as the "blob" of stratospheric air ([ST] > 10^{-1} kg/kg) between 600 and 800 hPa (Figure 7). This was related to the injection of stratospheric air into the troposphere down to 500 hPa around hour 24.

3.3.2. FLEXPART

[16] At JUN, too low [ST] values were obtained from the simulation around hour 67 when the maximum values of O_3 were recorded at the station (Figure 4). These low [ST] values were related to the input of stratospheric air simulated around hour 48 (Figure 5). During the second STT event, a tropopause lowering (down to 450 hPa in Figure 5) was simulated, showing low [ST] values (<10^{-3} kg/kg) at the measurement site. For CIM, very high values of [ST] were simulated by FLEXPART (up to 10^{-1} kg/kg) between hours 88 and 138 (Figure 6). The [ST] increase can be related to different inputs of stratospheric air (Figure 7). In fact, after a first stream around hour 24, an injection of high [ST] and low [SH] occurred from hour 48. After hour 72, a reservoir layer of [ST] was simulated between 500 and 750 hPa.

3.3.3. STOCHEM

[17] Both for JUN and CIM, STOCHEM revealed a tropopause lowering below 300 hPa. However, the simulated intrusion did not penetrate to lower levels and did not

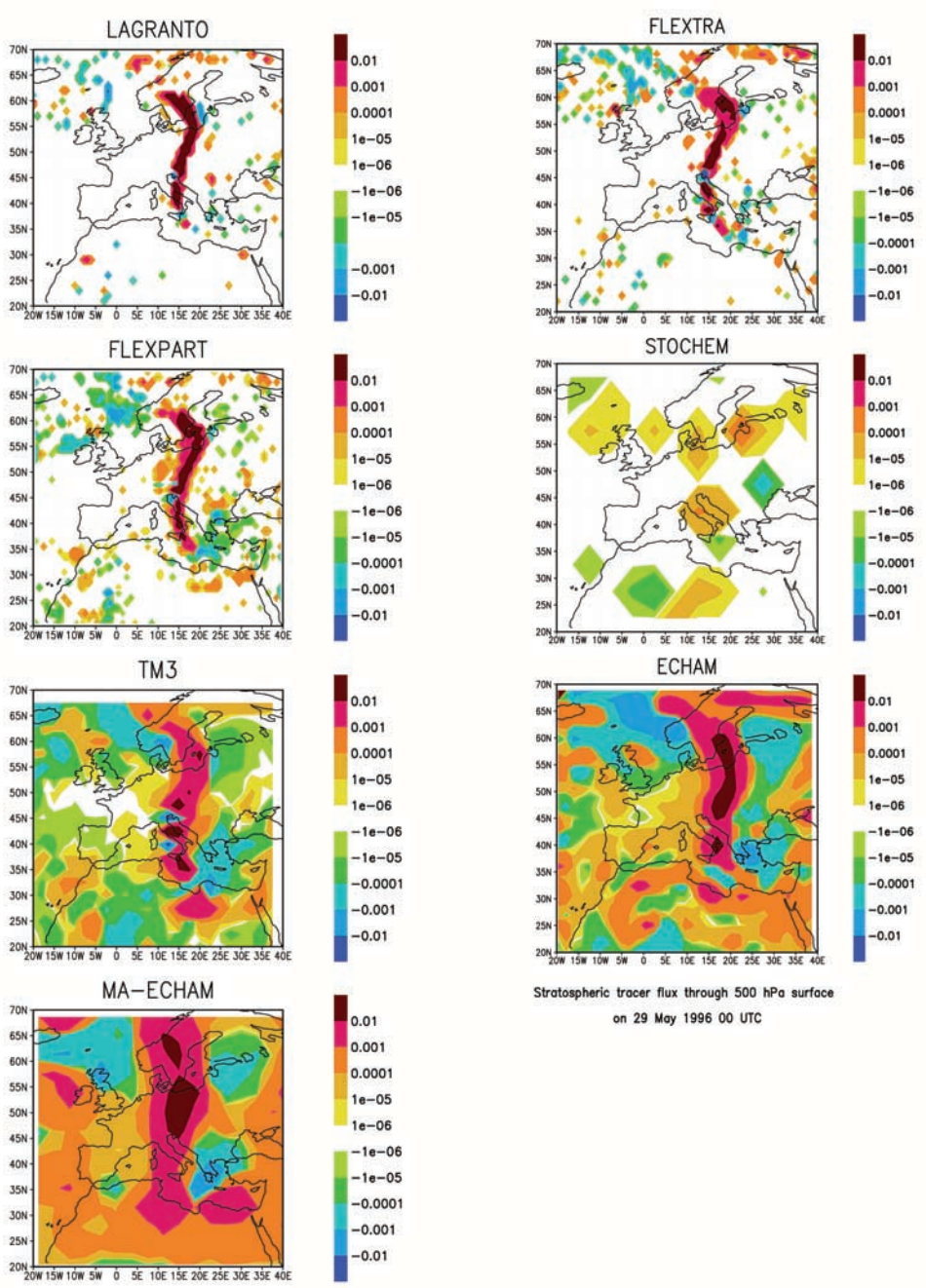

Figure 3. Latitude/longitude field for the 3-hour averaged stratospheric flux (kg m^{-2} s^{-1}) through the 500 hPa surface on 29 May 1996 at 1000 UTC. Positive (negative) values represent downward (upward) fluxes.

affect the mountain peaks (Figures 4, 5, 6, and 7), providing a too weak input of [ST] in the lower and middle troposphere. This is likely related to the fact that transport of the tracer was simulated by STOCHEM only with 100,000 particles distributed in the whole atmosphere. With such a small number of particles, the chances that a mesoscale intrusion event is missed are high.

3.3.4. TM3

[18] At JUN the highest [ST] ($\approx 10^{-2}$ kg/kg) were simulated at hour 39 at the time of a secondary O_3 peak (Figure 4). During the second STT event, only low [ST] was calculated below 600 hPa (Figure 5). At CIM, the highest [ST] values ($\approx 10^{-2}$ kg/kg) were calculated around hours 48 and 63, when two secondary O_3 peaks were recorded (Figure 6). The STT event recorded around hour 120 was not fully captured by TM3: only a broad but weak [ST] peak was centered at hour 96. These [ST] values were related to a stratospheric intrusion simulated around hour 48 (Figure 7). Although a tropopause lowering was present during the second STT event, high [ST] values were confined to above 600 hPa.

3.3.5. ECHAM4 and MA-ECHAM4

[19] At JUN the highest [ST] ($>10^{-1}$ kg/kg) was recorded ten hours before the strongest STT evidences, but still quite coincident (Figure 4). For ECHAM4, these [ST] were

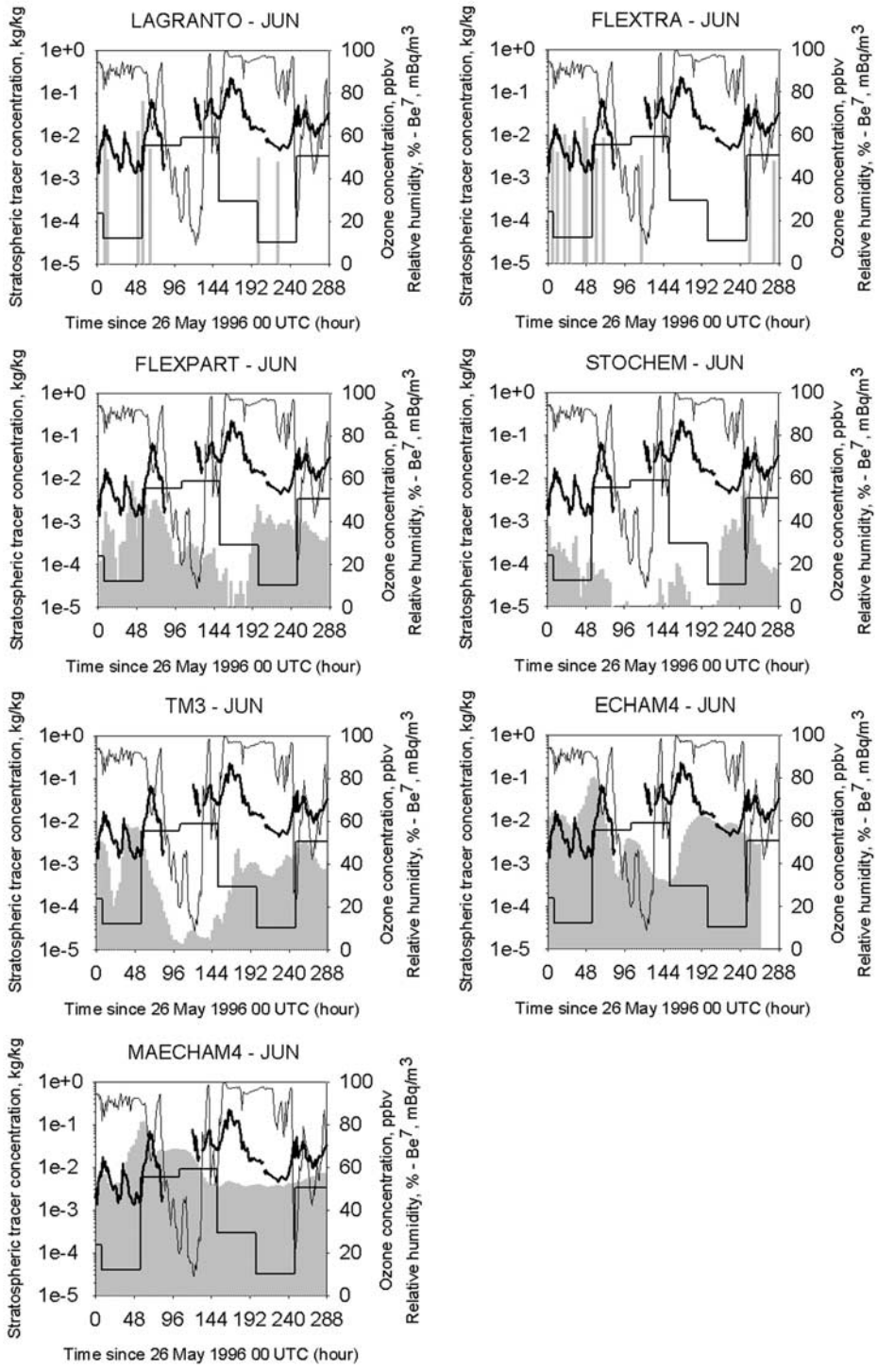

Figure 4. O_3 (thick line), RH (thin line) and Be-7 (noncontinuous line, multiplied by 5 in the right axis) recorded at JUN. In grey area are reported [ST] between 600 and 800 hPa for the different models.

related to the stratospheric air stream which reached the surface around hour 72, while for MA-ECHAM4 a large stratospheric influence persisted in the lower troposphere until hour 144. (Figure 5). During the whole second STT event, ECHAM4 simulated relatively high [ST] (average: 7×10^{-3} kg/kg) related with a broad tongue of stratospheric air below 600 hPa. For CIM, ECHAM4 and MA-ECHAM4 simulated the greatest stratospheric influence around hour 69 ([ST] > 10^{-1} kg/kg), when secondary O_3 peaks were recorded (Figure 6). While ECHAM4 simulated a secondary [ST] peak that partially overlapped with the O_3 peaks and RH decreases recorded around hour 110, MA-ECHAM4

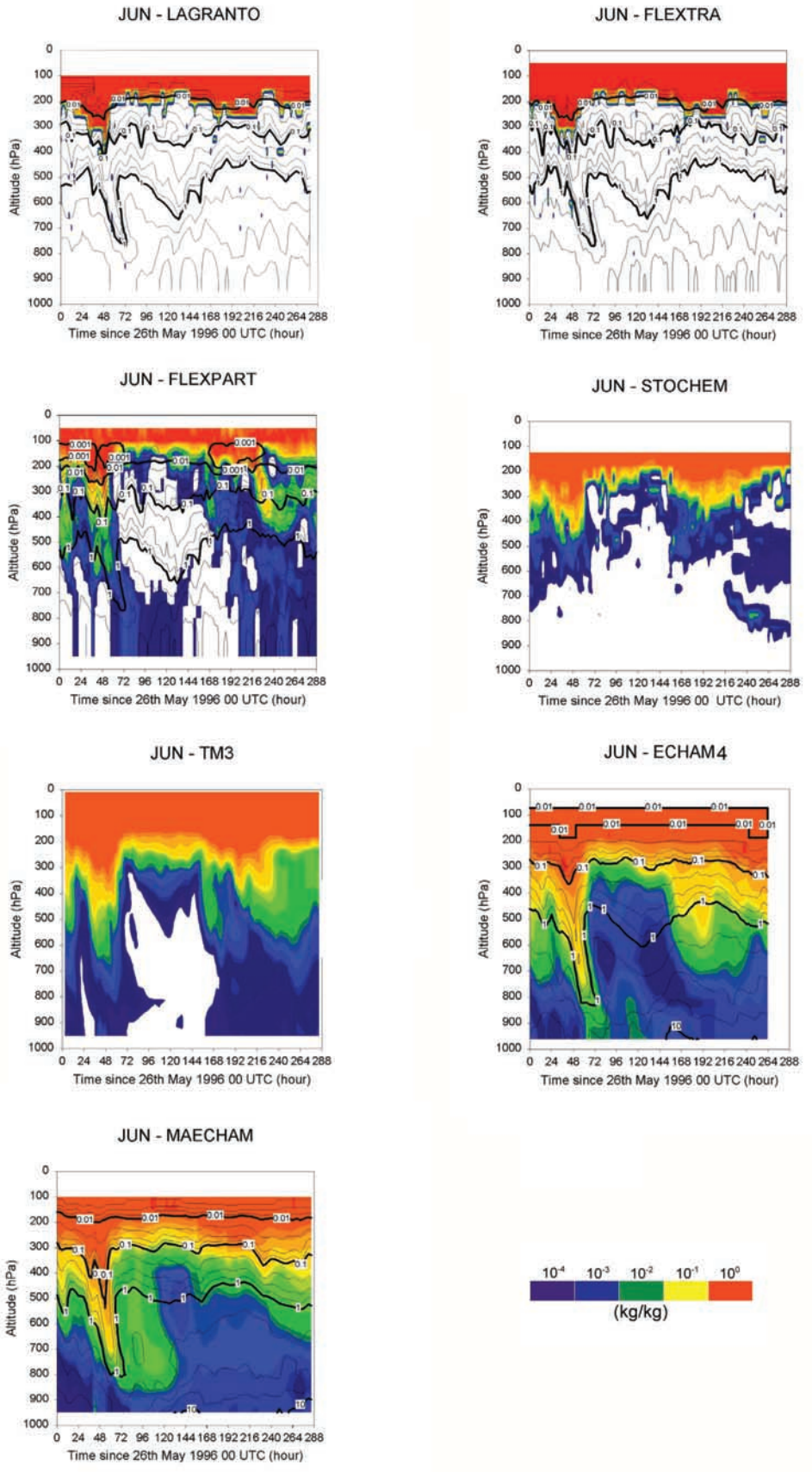

Figure 5. [ST] (filled area) and simulated SH (contour plot; kg/kg) time versus altitude at JUN for the different models.

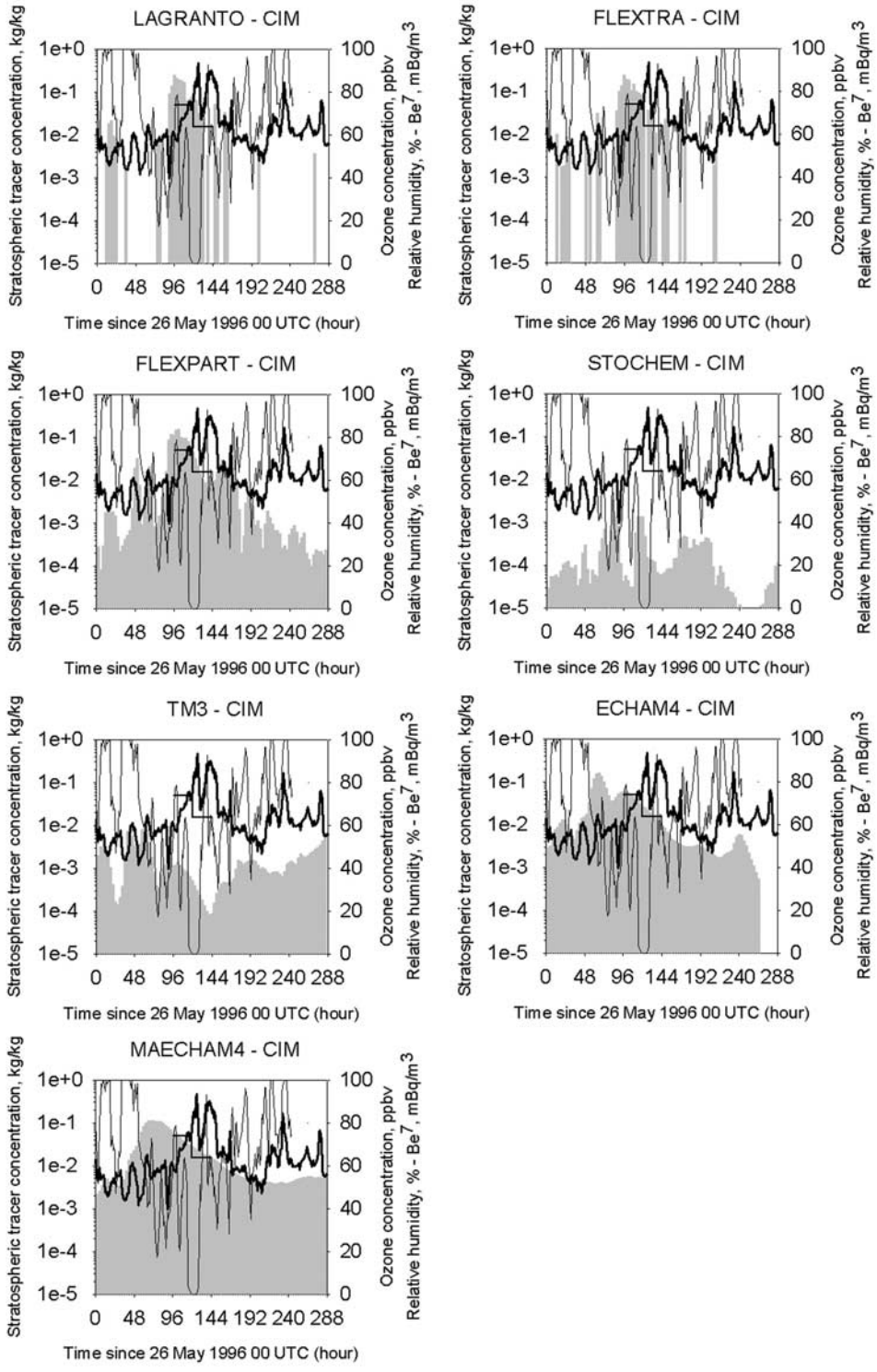

Figure 6. O_3 (thick line), RH (thin line) and Be-7 (noncontinuous line, multiplied by 5 in the right axis) recorded at CIM. In grey area are reported [ST] between 600 and 800 hPa for the different models.

calculated a very broad stratospheric intrusion which did not resolve the features of the event (Figure 7).

3.4. O_3, Be-7, and Be-10

[20] As previously reported, some of the models calculated the vertical profiles of O_3, Be-7 and Be-10 at the measurement sites: STOCHEM simulated both O_3 and radionuclides, ECHAM4 only O_3 and MA-ECHAM4 only Be-7 and Be-10 (see Table 3).

3.4.1. STOCHEM

[21] This model calculated tropospheric O_3 using a chemistry scheme involving oxidation of hydrocarbons up to C4 and isoprene. O_3 above the tropopause is relaxed with a 20 day e-folding time toward the monthly ozone climatology

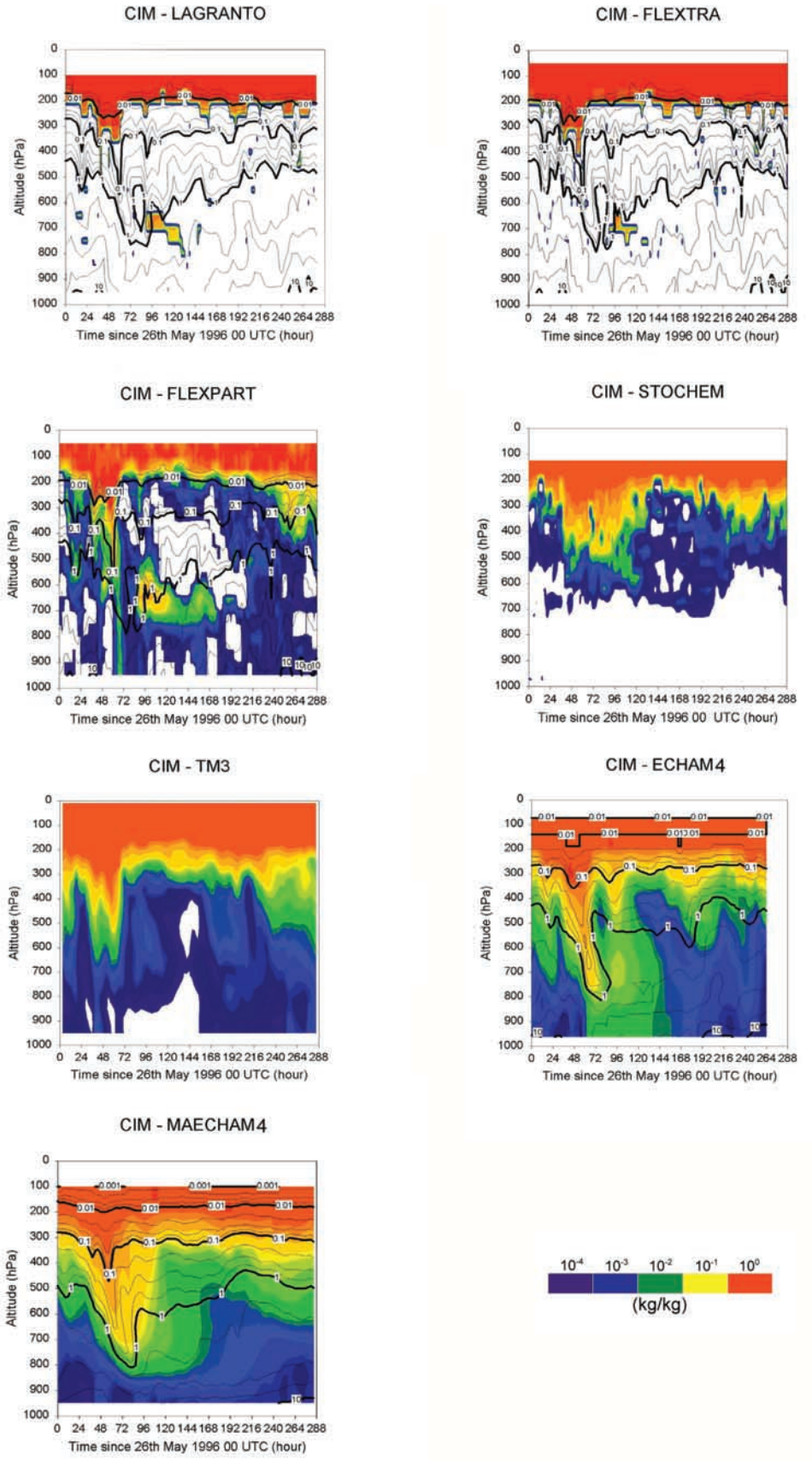

Figure 7. [ST] (filled area) and simulated SH (contour plot; kg/kg) time versus altitude at CIM for the different models.

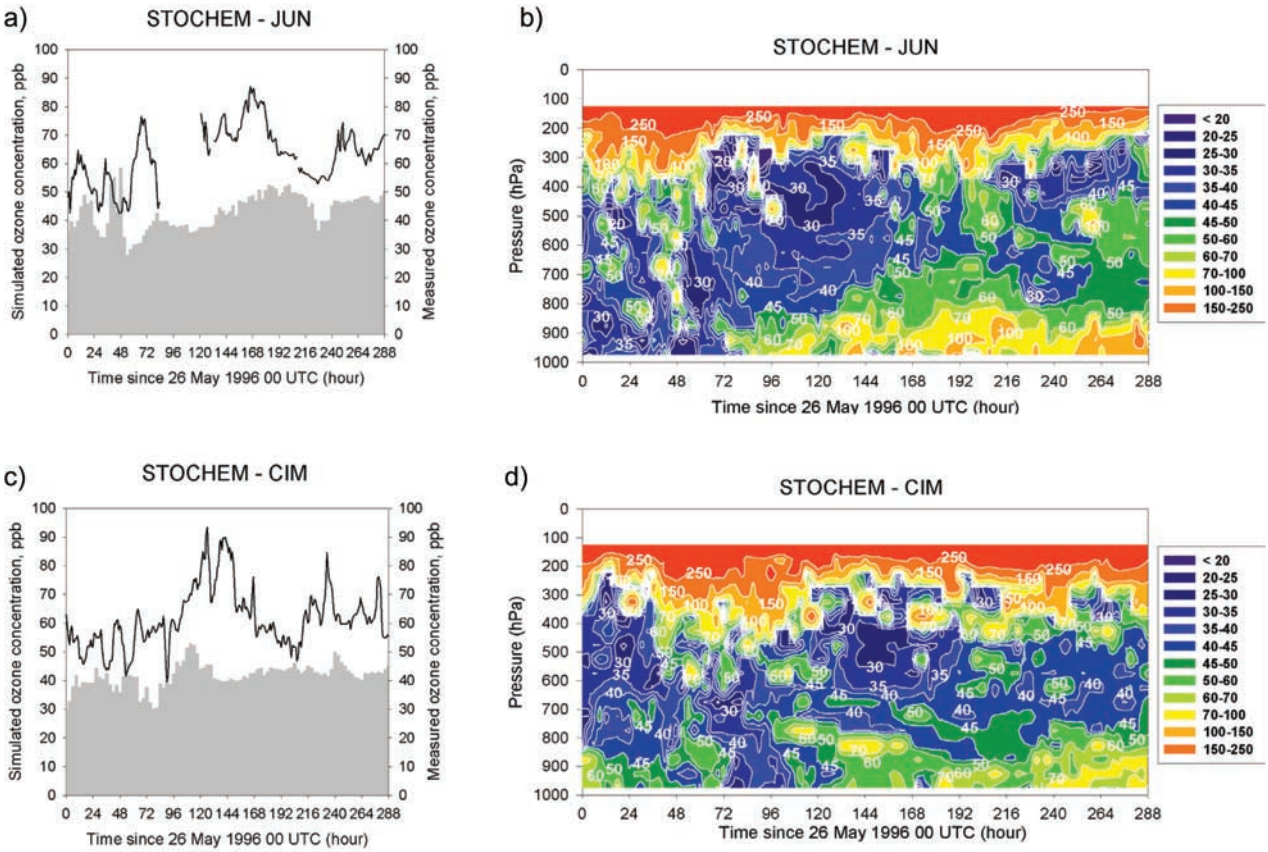

Figure 8. STOCHEM analysis. O_3 (thick line) at JUN (a) and CIM (c). Simulated O_3 between 600 and 800 hPa is reported in grey area. Plate b (d) represents the simulated O_3 (filled area; ppb) time versus altitude plot for JUN (CIM).

from *Li and Shine* [1995]. Low O_3 levels were predicted by this model at JUN (Figure 8a). STOCHEM calculated descending stratospheric O_3 both around hour 48 and during the second STT event (since hour 144), for which the model also simulated photochemical O_3 production in the lower troposphere (Figure 8b). Similar results were found for CIM (Figure 8c), where the main increase of stratospheric O_3 was simulated around hour 48 (Figure 8d), with high photochemical concentration after hour 138 (as described by *Bonasoni et al.* [2000]).

[22] Be-7 and Be-10 production rates are used in STOCHEM according with *Masarik and Beer* [1999]. STOCHEM underestimates the measured values at JUN and ZUG (Figures 9a and 9c). The 8 mBq/m^3 Be-7 concentration, indicated by *Reiter et al.* [1983] as typical values to trace STT events, was simulated only at about 400–500 hPa (Figures 9b and 9d). Also the highest Be-10 were underestimated by STOCHEM (Figure 10). An explanation for the Be-7 and Be-10 underestimation, could be found in the rather crude scavenging parameterization applied.

3.4.2. ECHAM4

[23] The model used a CBM4 chemistry scheme to calculate O_3, which is advected by a semi-Lagrangian transport scheme. Stratospheric O_3 is parameterized by a 2D stratospheric chemistry model and by an O_3-potential vorticity scheme in the lower stratosphere (see also G. J. Roelofs et al., Intercomparison of tropospheric ozone models: Ozone transport in a complex tropopause folding event, submitted to *Journal of Geophysical Research*, 2003, hereinafter referred to as Roelofs et al., submitted manuscript, 2003). For JUN, the O_3 peak at hour 67 (Figure 11a) was simulated as transported downward by stratospheric air rich in O_3 (Figure 11b). Also during the second event the simulated O_3 was in good agreement with measurements, both having maximum values of about 80–90 ppb. For CIM (Figure 11c), ECHAM4 simulated too high O_3 concentrations and they occurred too early, compared with the measurements. This is partly due to the coarse resolution of ECHAM4: the simulated peaks in stratospheric ozone at JUN and CIM occurred at the same time (Figures 11a and 11c), while in the measurements the peak at CIM occurred two days after the one at JUN.

3.4.3. MA-ECHAM4

[24] Be-7 and Be-10 production are simulated as explained by *Land and Feichter* [2003]. At JUN, the peak values of 11 mBq/m^3 and 10 mBq/m^3 shown by measurements and model results (Figure 12a), were related to the first input of stratospheric air (hour 24–72, Figure 12b). On average the model underestimates Be-7 concentration. At ZUG (Figures 12c and 12d), where the radionuclide sampling was carried out with 24 hour resolution, the measured and simulated series showed a very good agreement (par-

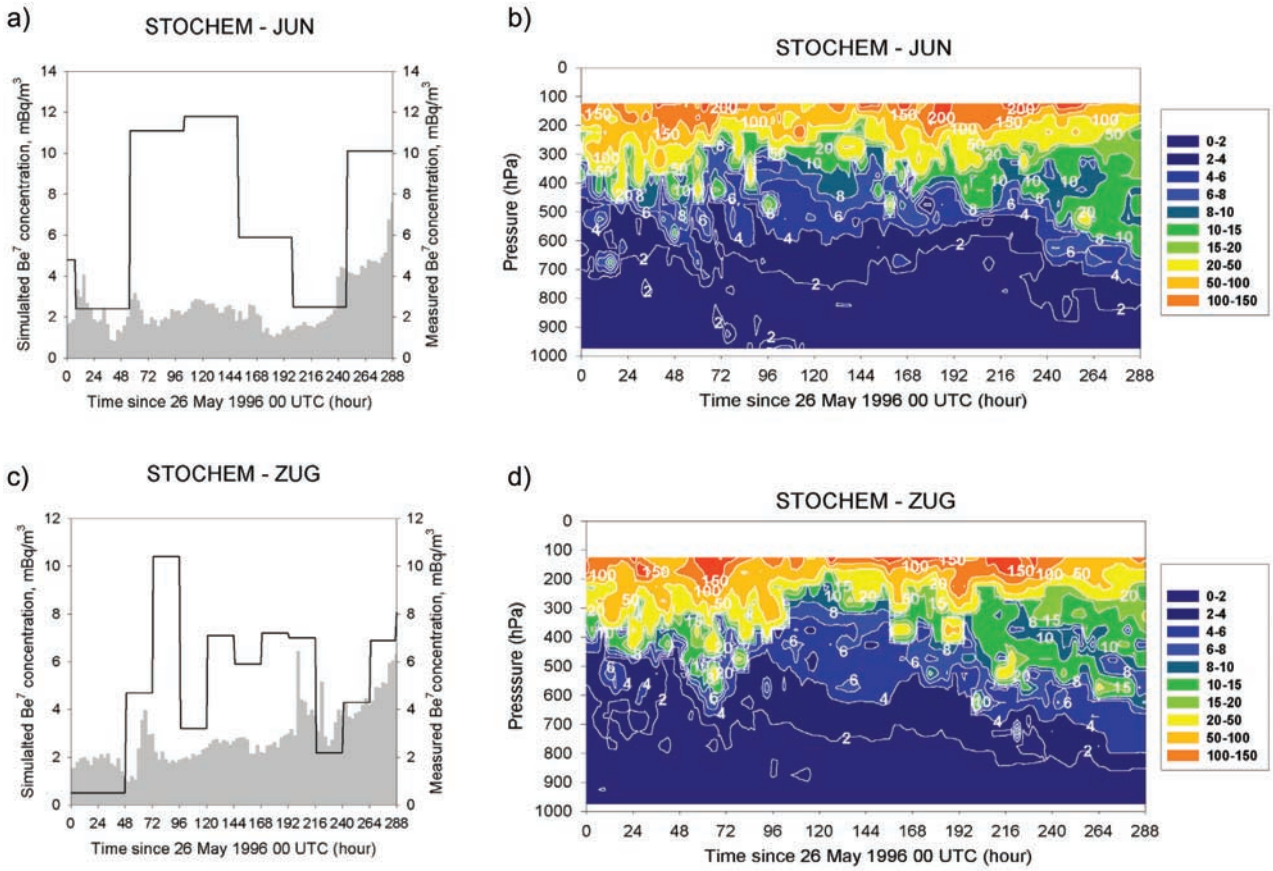

Figure 9. STOCHEM analysis. Be-7 (thick line) at JUN (a) and ZUG (c). Simulated Be-7 between 600 and 800 hPa is reported in grey area. Plate b (d) represents the simulated Be-7 (filled area; mBq/m^3) time versus altitude plot for JUN (ZUG).

ticularly during the peak event around hour 72). For Be-10 (Figure 10), a good agreement is found between simulated and measured data.

3.5. Stratospheric Tracer Concentrations at Atmospheric Sounding Stations

[25] In this section we compare simulated (i.e. [ST], O_3, SH) with measured vertical profiles (i.e. O_3, RH, SH). For this comparison, we use data from PAY, HOH and GAR, where many vertical profiles were available (see Table 2).

[26] The tropopause folding that developed during the first STT event was studied in particular between hours 48 and 104. During this period PAY soundings recorded dry air (RH < 30%, SH < 1 kg/kg) between 500 and 900 hPa, and especially around 600 hPa where O_3 was enhanced (90 ppb) in the ozone-sounding carried out at hour 60 (Figure 13).

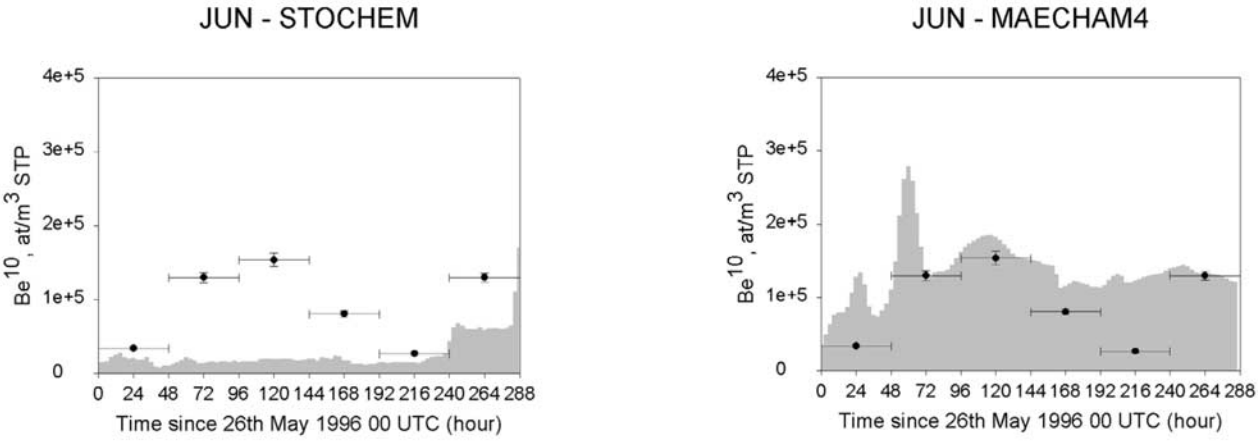

Figure 10. Comparison between the measured (scatter crosses) and simulated (grey area) Be-10.

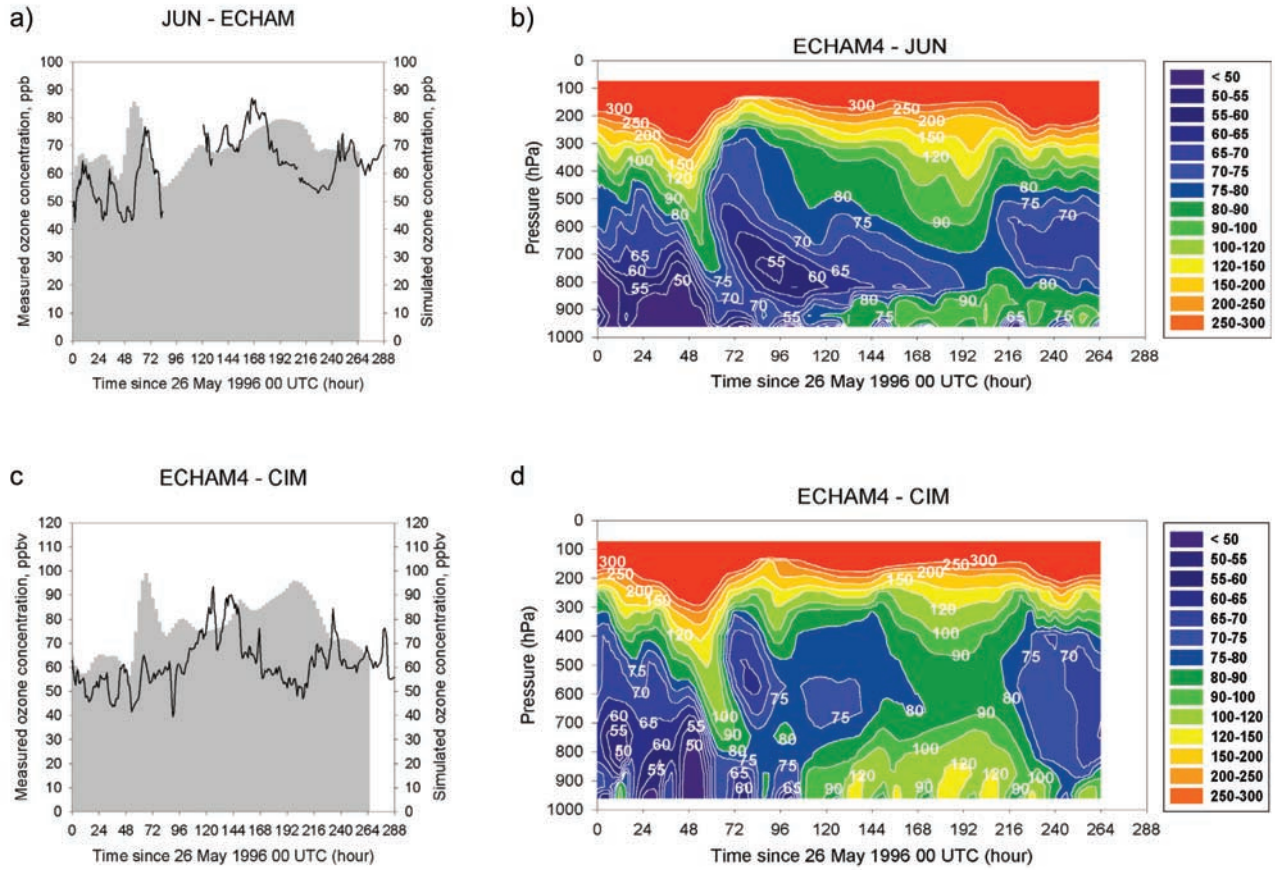

Figure 11. ECHAM4 analysis. O_3 (thick line) at JUN (a) and CIM (c). Simulated O_3 between 600 and 800 hPa is reported in grey area. Plate b (d) represents the simulated O_3 (filled area; ppb) time versus altitude plot for JUN (CIM).

The following ozone-sounding (hour 84), had a more complex structure with two well-defined layers (around 550 and 850 hPa) with high O_3 (up to 80 and 75 ppb) and low RH (30%). From hour 80 to hour 104, descent of stratospheric air to below 4 km was seen in the ozone lidar data at GAR (air mass marked ST in Figure 14) with concentrations above 60 ppb [*Eisele et al.*, 1999].

[27] During the second STT event (hour 204 and 252), the ozone-soundings recorded at PAY showed different dry and O_3-rich layers, as reported in Figure 13.

3.5.1. LAGRANTO and FLEXTRA

[28] The models showed similar behaviors simulating the STT event. Around hour 48, both models showed a lowering of the tropopause height for PAY (Figure 15). However, even if they provided simulated SH according to observations, only LAGRANTO showed not negligible [ST] around 600 hPa at hour 60 (Figure 13).

[29] During the second STT event, a lowering of the tropopause level down to 300 hPa was seen (Figure 15). At hour 204, LAGRANTO placed [ST] > 10^{-2} kg/kg at almost the same altitude of observed O_3 peak (350–550 hPa). At hour 252, the two models simulated noncontinuous [ST] around 400 hPa, where an O_3 peak was recorded (Figure 13).

3.5.2. FLEXPART

[30] Between hours 48 and 72, FLEXPART simulated for PAY a tongue of stratospheric air down to 600 hPa (Figure 15). At hour 60 the model placed [ST] > 10^{-2} kg/kg around 600 hPa, according to O_3 and RH measurements (Figure 13). After 24 hours, the dry and O_3-rich air mass at 550 hPa, was totally missed. This can be explained looking at the lidar sequence carried out at GAR. In fact, after the tropopause fold, an Atlantic air mass (MA in Figure 14) with low O_3 (below 50 ppb) crossed the measurement site at an altitude between 2 and 7 km (≈760–370 hPa) [*Eisele et al.*, 1999]. On the other hand, the elevated O_3 concentrations present in the troposphere (above 4 km), has been related to the advection of polluted air from USA [*Trickl*, 2003]. Thus, the moist and O_3-poor layer around 700 hPa and the upper dry layer and rich in O_3 recorded at PAY (≈350 km west of GAR) around hour 84, could be associated with the Atlantic and USA air masses identified around hour 98 by lidar. Similarly, the high O_3 recorded by ozone-sounding profiles above 750 hPa at hour 132 (PAY) could be explained. Thus, also the low RH as well as the high Be-7 and Be-10 recorded at JUN during the middle of the case study (section 3.3), could be associated to upper-tropospheric advection of air masses having crossed the Atlantic Ocean. At GAR, below 4–5 km, the agreement between the FLEXPART results and the lidar measurements was not totally satisfying as low [ST] values (<10^{-3} kg/kg; Figure 16) were calculated.

[31] During the second STT event, the model did not capture the stratospheric air recorded at PAY at hour 204,

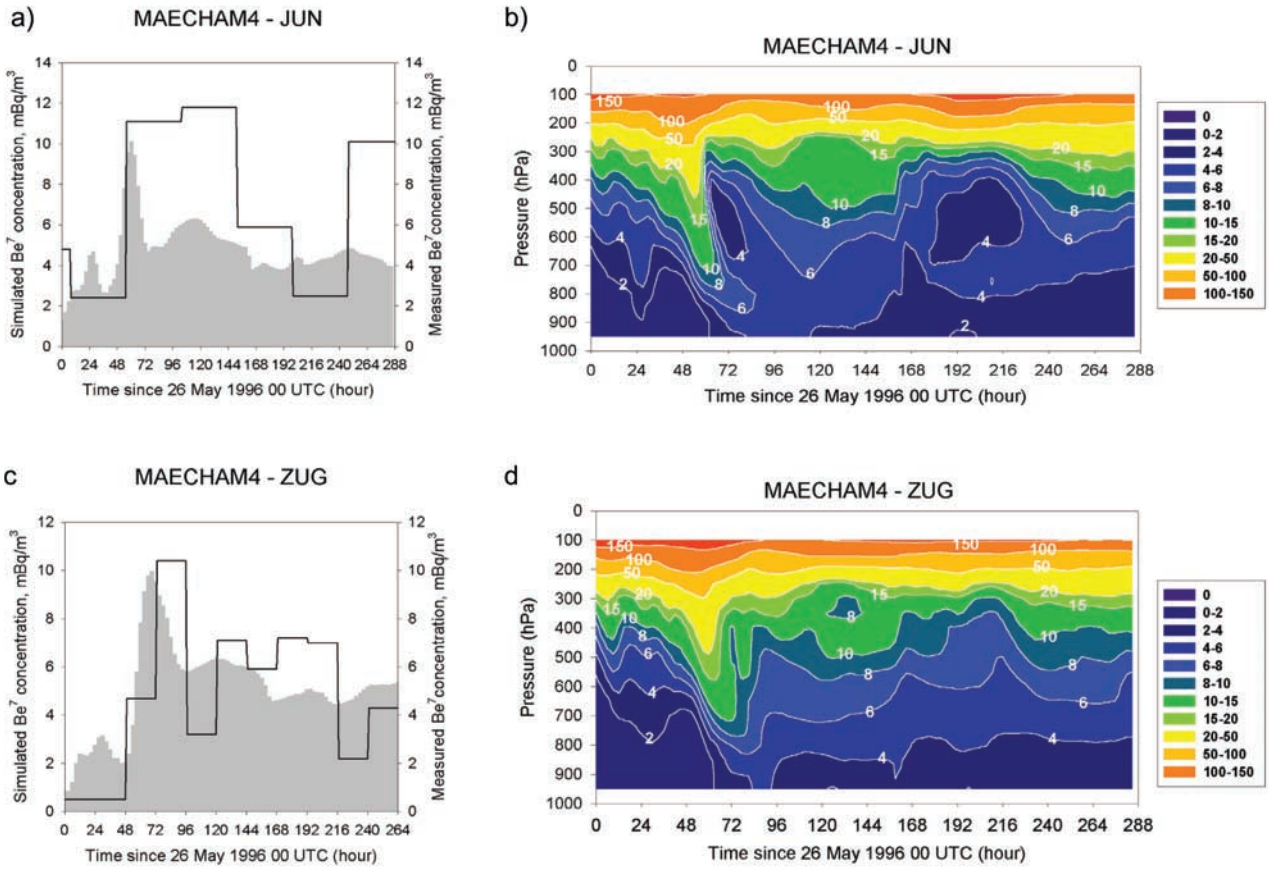

Figure 12. MA-ECHAM4 analysis. Be-7 (thick line) at JUN (a) and ZUG (c). Simulated Be-7 between 600 and 800 hPa is reported in grey area. Plate b (d) represents the simulated Be-7 (filled area; mBq/m^3) time versus altitude plot for JUN (ZUG).

but it simulated a pronounced stratospheric influence between 350 and 550 hPa at hour 252 (Figure 13).

3.5.3. STOCHEM

[32] Even if showing a clear lowering in the tropopause level (Figure 15), the STOCHEM model showed too low [ST] to explain the RH and the O_3 recorded by measurements (Figure 13). Similarly, for GAR a weak input of [ST] ($<10^{-3}$ kg/kg) was present at too high altitude (between 4 and 6 km) to overlap with the stratospheric O_3 revealed by lidar (Figure 16).

3.5.4. TM3

[33] At PAY, a well-defined intrusion of [ST] ($>10^{-2}$ kg/kg) started at hour 24 and reached, after strong mixing and dilution, low levels (Figure 15). In spite of experimental evidences, around hour 60, TM3 simulated stratospheric air ([ST] $> 10^{-2}$ kg/kg) only above 600 hPa, and around hour 84 the [ST] was small between 900 and 800 hPa (Figure 13). At GAR the agreement between the TM3 results and the lidar measurements was not satisfying below 4 km, where low [ST] values ($<10^{-3}$ kg/kg) was calculated by the model (Figure 16). The second STT event was simulated by TM3 above 500 hPa ([ST] $> 10^{-2}$ kg/kg) without capturing the atmospheric layering recorded at hour 204 (Figure 13). After 48 hours, even if somewhat lower than observed, a quite broad [ST] peak (10^{-2} kg/kg) was simulated at 500 hPa in agreement with the measured O_3 peak recorded.

3.5.5. ECHAM4 and MA-ECHAM4

[34] Around hour 60 the models simulated SH < 1 kg/kg at 800 hPa level (Figure 15), well in accordance with the ozone-sounding data. At this time, they simulated over PAY a thick stratospheric layer, but for ECHAM4 a lower altitude than observed (Figure 13). After 24 hours, ECHAM4 located this layer around 850 hPa, whereas MA-ECHAM4 simulated a too broad intrusion weak in agreement with the layering recorded by measurements. At GAR, [ST] $> 10^{-2}$ kg/kg were related to the tropopause folding (Figure 16). However, an excessive spread of stratospheric air was found. This was more evident for MA-ECHAM4, for which the high [ST] did not capture all the features of the event.

[35] During the second STT event, both models did not capture the layering recorded by the measurements. Particularly, they simulated at PAY a too deep stratospheric influence since hour 204 (Figure 13).

3.6. O_3 at Atmospheric Sounding Stations

[36] In order to evaluate the simulated O_3, the averaged deviation (ΔO_3) of the simulated from measured values inside a "low tropospheric layer" (between the surface and

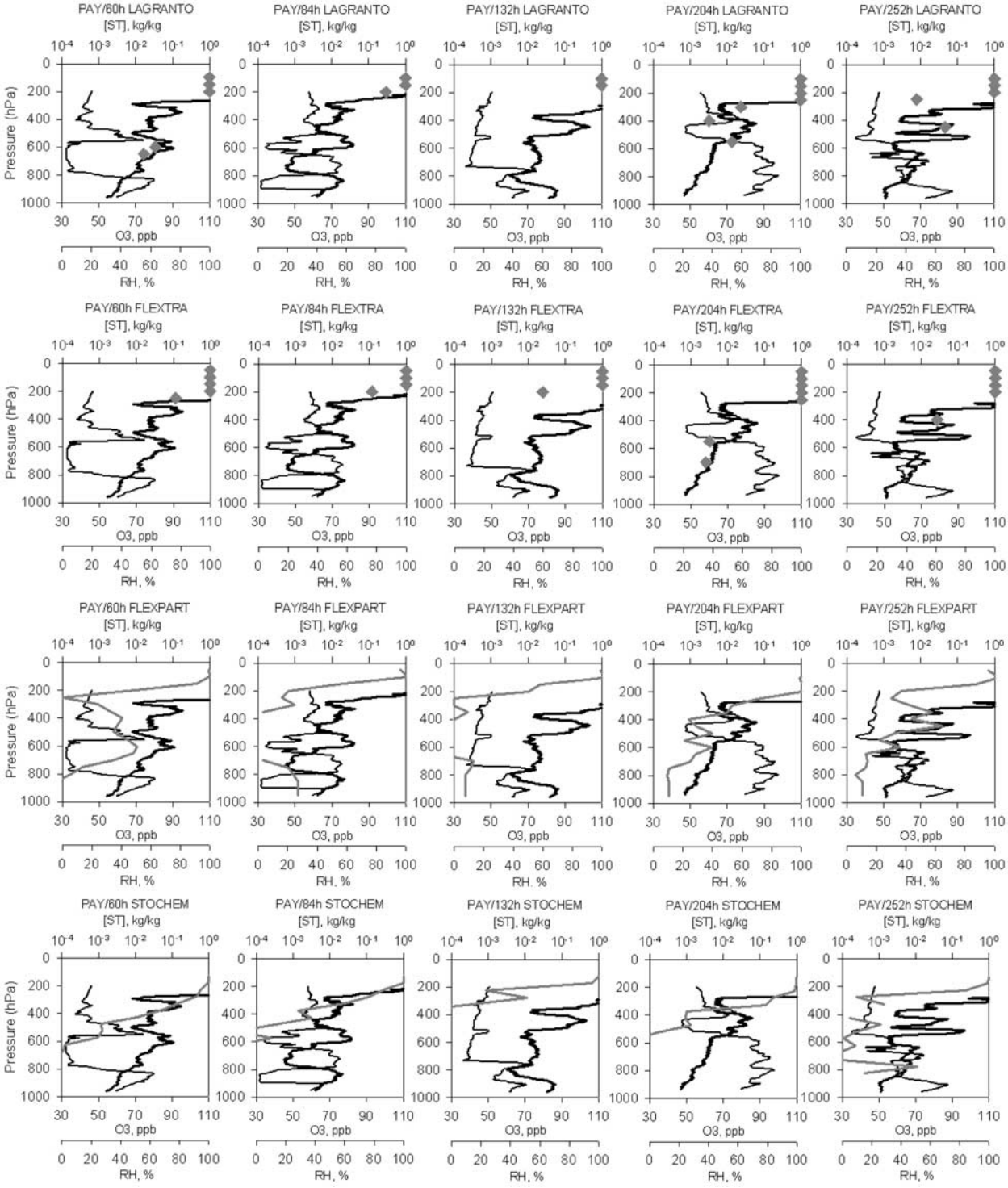

Figure 13. Observed O_3 (thick line) and RH (thin line) together with average [ST] (gray line) at PAY. The [ST] average was obtained by averaging the three successive profiles simulated around the O_3-sounding.

800 hPa) and an "upper tropospheric layer" (between 800 and 300 hPa) is considered. The results are reported in the Table 4.

3.6.1. STOCHEM

[37] For PAY and HOH, this model simulated an underestimation of O_3 between 800 and 300 hPa, while a clear surplus of photochemical O_3 was simulated inside the "low tropospheric layer" during the second STT event (Table 4). Particularly, during the first STT event the intrusion features were not completely reproduced at PAY (Figure 17). The O_3 underestimation appeared clearly also comparing STOCHEM with lidar profiles at GAR. At hours 204 and 252,

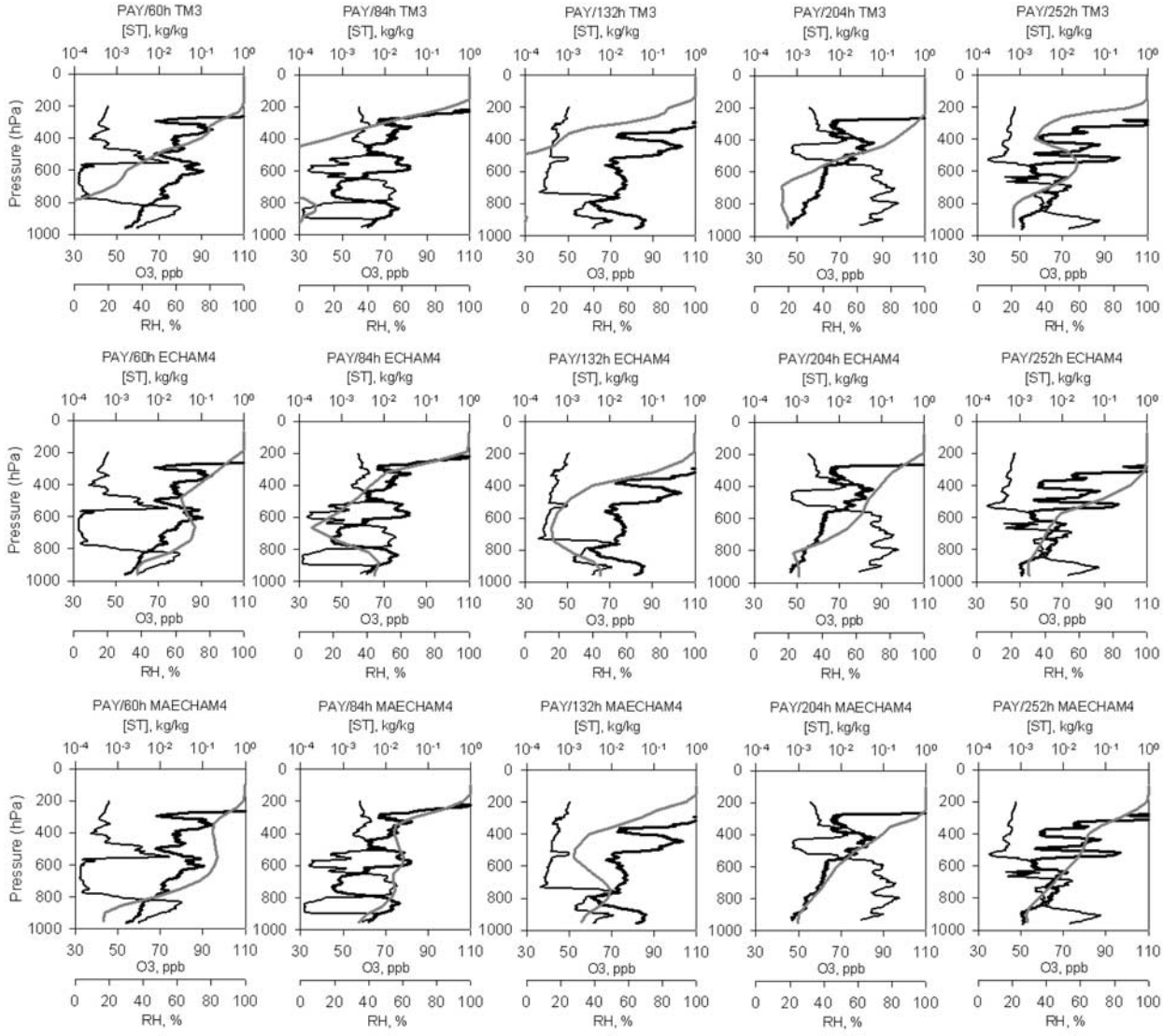

Figure 13. (continued)

STOCHEM placed O_3 peaks at quite the correct altitudes, and it approached the O_3 levels observed at PAY.

3.6.2. ECHAM4

[38] During the first STT event, ECHAM4 simulated O_3 values similar to those recorded at PAY and HOH ($|\Delta O_3| <$ 8 ppb). Particularly, the O_3 layering calculated by ECHAM4 at PAY was quite realistic (Figure 17). In good agreement with profile recorded at hour 132, the model simulated high O_3 moving downward from the upper troposphere between hours 72 and 144. For GAR, ECHAM4 simulated O_3 at 60–70 ppb within the folding. Moreover, also the low O_3 within the marine air mass ($O_3 < 60$ ppb), and the transport episode from North America ($O_3 > 70$ ppb) were identified quite well (Figure 17).

[39] During the second STT event, on average high O_3 was simulated at PAY (see Table 4), with the ozone-pause simulated below the observed altitude. Particularly, below 800 hPa, it is the contribution of the photochemical production (since hour 144; upper plate 17) which contributes largely to exceed the observed data ($\Delta O_3 > 24$ ppb). Similar O_3 values were simulated for HOH, except that results were better between 800 and 300 hPa (Table 4).

4. Discussion and Conclusion

[40] In order to evaluate seven models used in the STACCATO project to study STE, a detailed validation exercise was carried out during a stratospheric intrusion event. The results of an intercomparison of these models are reported in a companion paper [*Meloen et al.*, 2003], while in this paper a comparison between model and measurement data is presented. Two trajectory models (LAGRANTO and FLEXTRA), two Lagrangian transport model (FLEXPART and STOCHEM), one Eulerian transport model (TM3) and two global circulation model (ECHAM4 and MA-ECHAM4) provided vertical profiles of an ''idealized'' stratospheric tracer during a 12-day case study period (26 May 1996 to 7 June 1996). In addition, some of these models also provided vertical profiles of water vapor, O_3, Be-7 and Be-10 concentra-

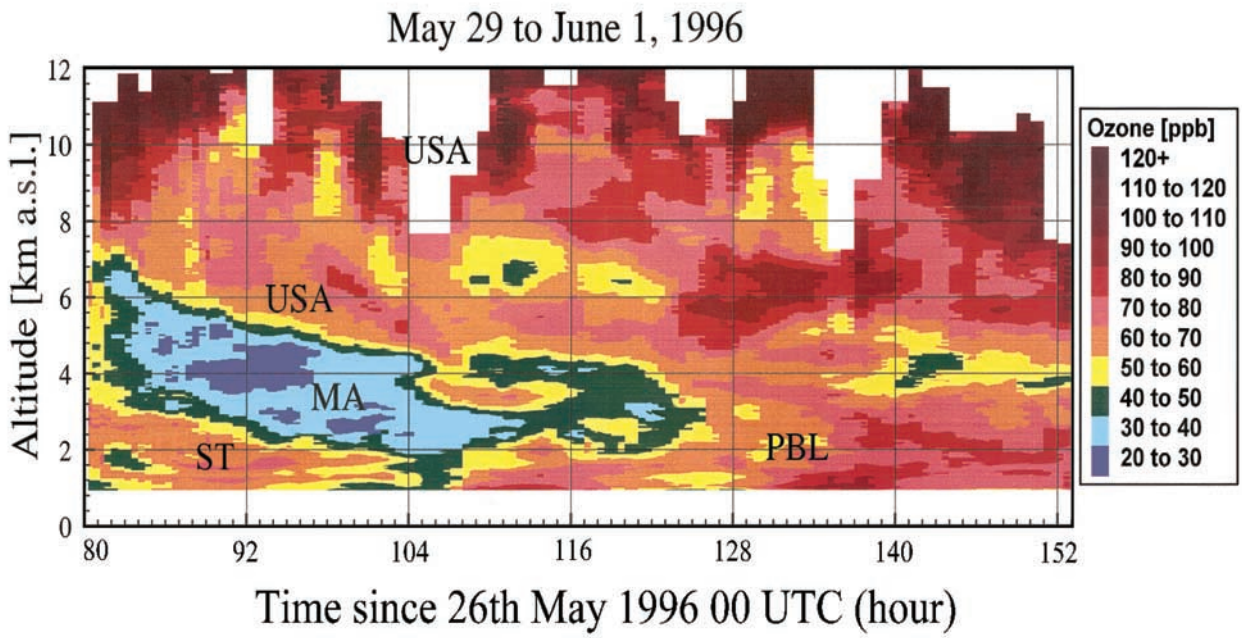

Figure 14. Time versus height plot for O_3 recorded since 29 May to 1 June 1996 at GAR (lidar). Different structures and air masses have been highlighted: tropopause folding (ST); marine air masses (MA); North America air masses (USA); boundary layer air masses (PBL). From *Eisele et al.* [1999].

tions. The model results have been evaluated using an extensive set of measurements, including satellite images, ozone-soundings and measurements performed at mountain stations.

[41] LAGRANTO, FLEXTRA and FLEXPART showed similar features. The analysis of stratospheric tracer fluxes through the 500 hPa level showed a thin filament with high downward fluxes of the stratospheric tracer. However, LAGRANTO and FLEXTRA mostly showed sporadic and non continuous [ST] increases below 300 hPa. This can be explained because LAGRANTO and FLEXTRA were the only models that had no parameterization for convection and turbulence. Nevertheless, these models, together with FLEXPART, were the only ones that identified a very large input of stratospheric air over CIM and CAP (not shown). FLEXPART showed higher simulated tracer concentrations in the middle-lower troposphere than the trajectory methods. A more detailed spatial and temporal analysis found good agreement with measurement data and permitted to describe the descent of the different stratospheric air streams down to the middle troposphere. However, compared with recorded data, an underestimation of stratospheric air was found approaching the surface (sections 3.3 and 3.5). As reported by Meloen et al. (submitted manuscript, 2002), the time series of the domain-averaged [ST] at 700 hPa for LAGRANTO, FLEXTRA and FLEXPART were characterized for the almost same behavior and absolute values. This could suggests that the great part of input of stratospheric air in the lower troposphere was confined, for trajectory models, inside well localized areas.

[42] The STOCHEM model underestimated STT during this event (particularly during the first part of the case study). In fact, at the 500 hPa level, STOCHEM captured only partially the shape of the stratospheric streamer seen in WV images. Analyzing [ST] and simulated O_3 profiles, STOCHEM showed a decrease in the tropopause height, but the modeled intrusion was weaker than recorded. This behavior could be explained by the relatively small number of air parcels used by the model to simulate the transport [*Meloen et al.*, 2003]. However, a further intercomparison (Roelofs et al., submitted manuscript, 2003), displayed satisfactory vertical resolution and concentration levels of simulated O_3 for STOCHEM during another intrusion episode. Thus, the crude meteorological assimilation scheme used for this case study, could be responsible for the underestimation of the event. In fact, the adoption of an improved assimilation scheme led to a significant change in the model results, better in agreement with other models and measurement data (Figure 18). On the other hand, the low Be-7 and Be-10 values, may be due to the scavenging parameterization being too simple.

[43] TM3 presented a quite realistic description of the event both in the upper (section 3.2) and middle troposphere (sections 3.3 and 3.5). These results were probably due to the low diffusivity of the tracer advection scheme used by TM3. Moreover, TM3 is an off-line model and therefore relatively less influenced by variations of the vertical wind fields. However, TM3 showed only low [ST] in the lower troposphere (below 600–700 hPa) during STT episodes. This can be an effect of the relatively coarse horizontal resolution adopted.

[44] ECHAM4 and MA-ECHAM4 captured the downward motion of stratospheric air in the lower troposphere (section 3.3), but simulated an elevated [ST] background in the troposphere, not seen in the measurements, during the whole case study. As highlighted in the companion paper [*Meloen et al.*, 2003], ECHAM4 and MA-ECHAM4 are

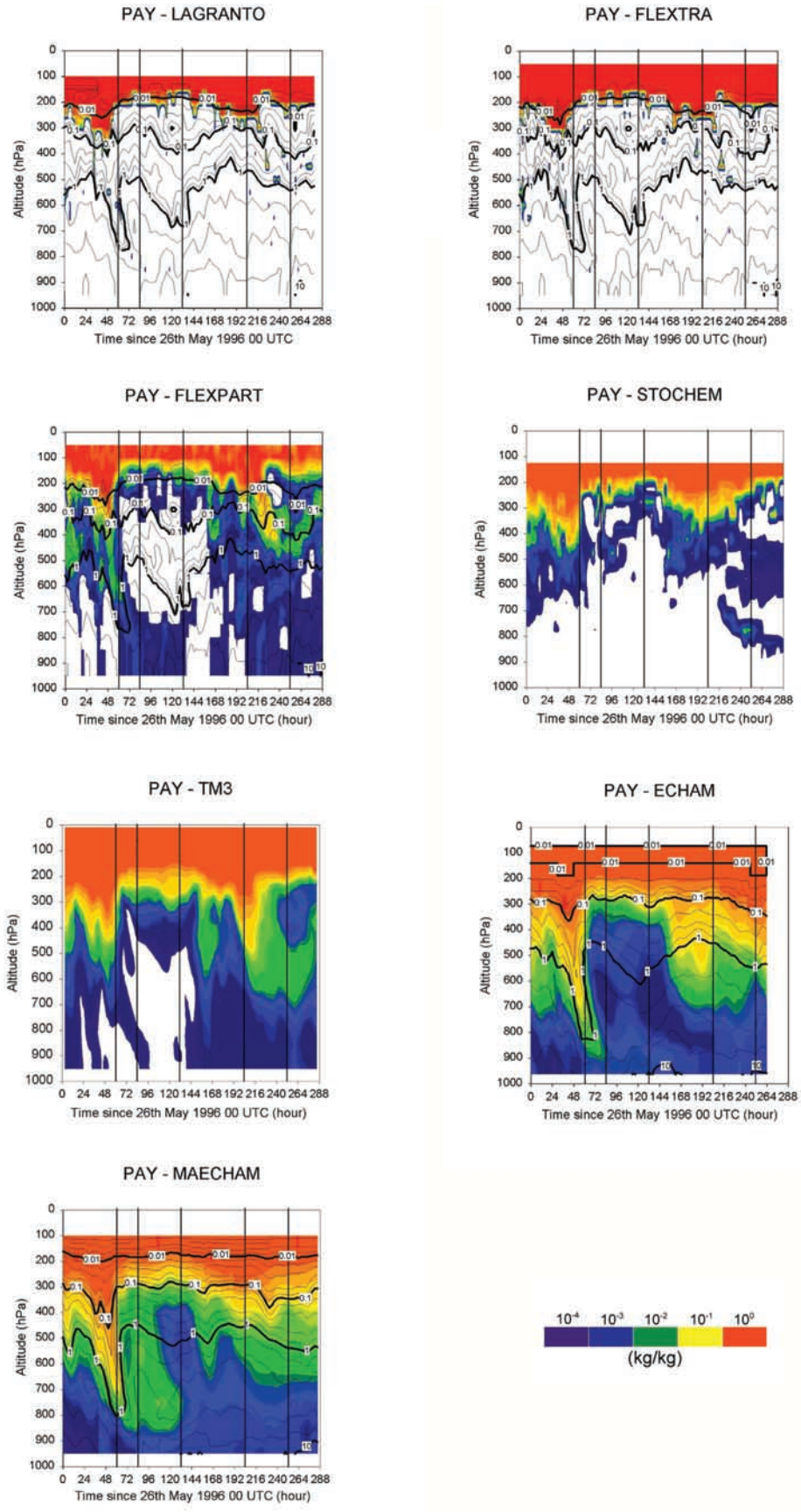

Figure 15. [ST] (filled area) and simulated SH (contour plot; kg/kg) time versus altitude at PAY for the different models. The vertical bar point-out the time for which ozone sounding are available.

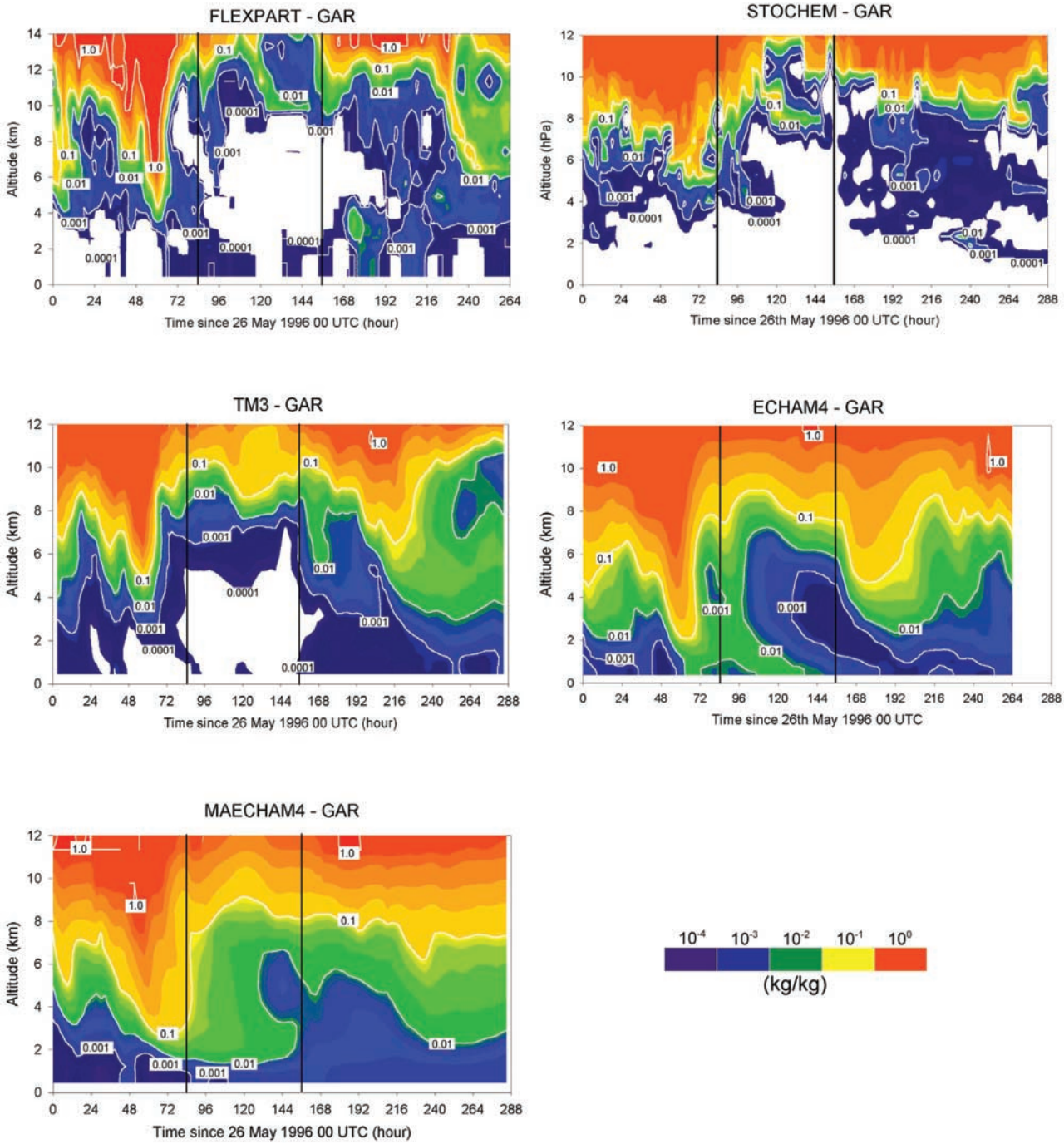

Figure 16. [ST] (filled area) time versus altitude at GAR for the different models. The vertical bar point-out the time-window for which lidar measurements are available.

Table 4. Average Deviation[a] of Simulated Values From Measured Values of O_3 Inside the "Low Tropospheric Layer" (<800 hPa) and the "Upper Tropospheric Layer" (800–300 hPa) Along the Vertical Profile at PAY and HOH

		ΔO_3 PAY					ΔO_3 HOH			
Model	Layer	hh: 60	hh: 84	hh:132	hh: 204	hh: 252	hh: 78	hh: 126	hh: 198	hh: 246
STOCHEM	<800 hPa	−28.3	−21.2	−2.2	+31.7	+22.1	−31.0	−16.5	+23.3	+15.1
	800–300 hPa	−36.6	−23.9	−45.4	−12.4	−25.8	−18.3	−44.7	−47.0	−32.2
ECHAM	< 800 hPa	−0.7	−3.4	−1.5	+32.4	+24.1	−3.0	−2.5	+32.6	+43.2
	800–300 hPa	−0.5	+2.6	−3.7	+20.8	+21.3	+7.6	+3.5	+12.8	−1.0

[a] ΔO_3 in ppb.

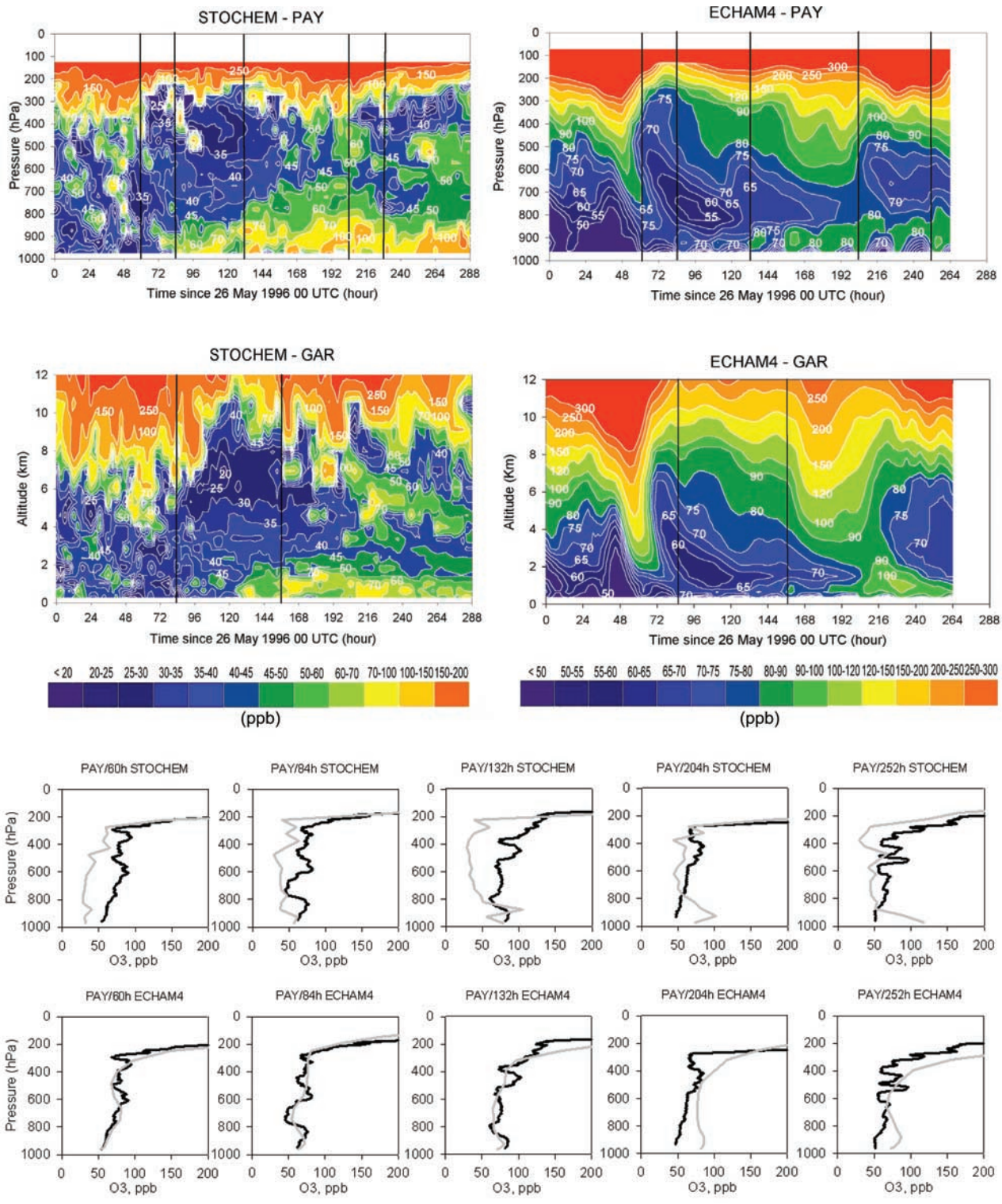

Figure 17. Upper plate: simulated O_3 (filled area) time versus altitude at PAY and GAR. The vertical bar point-out the time-window for which ozone sounding (at PAY) and lidar measurements (at GAR) are available. Bottom plate: observed (black line) and simulated (grey line) O_3 at PAY.

strongly influenced by numerical diffusion and by a large variability of the vertical winds due to their being on-line models. This can be the reason why these models provided high [ST] values throughout the troposphere. In fact their ozone and radionuclides simulations, were in much better agreement with the measurements because these tracers do not have strong gradient at the tropopause and are, thus, less affected by numerical diffusion which appears causing a loss in the spatial and temporal resolution in STT simulation. This was more evident for MA-ECHAM4 having a

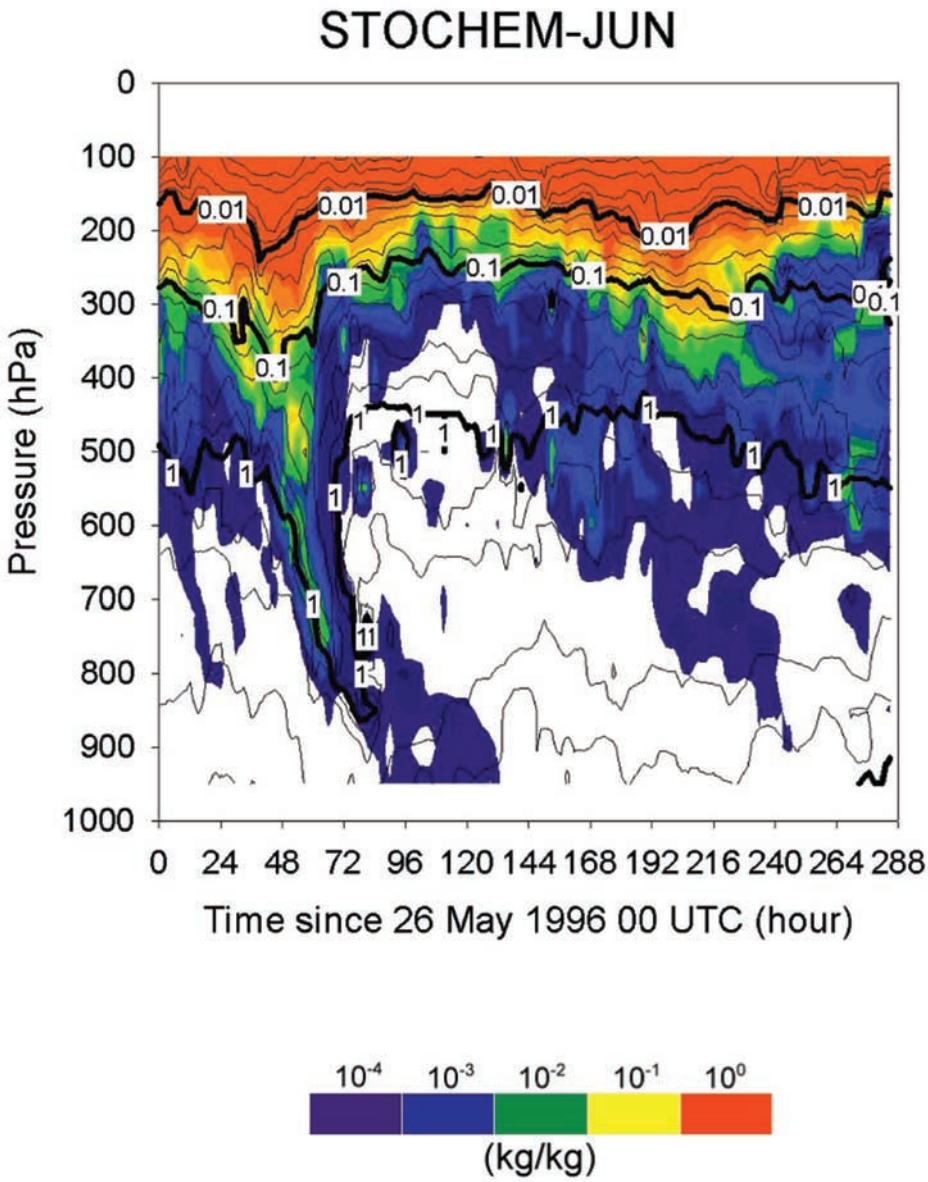

Figure 18. [ST] (filled area) and simulated SH (contour plot; kg/kg) time versus altitude at JUN for STOCHEM when the new meteorological parameterisation is applied.

less diffusive advection scheme but a coarser horizontal resolution than ECHAM4. This suggests that good horizontal resolution is important to reduce the numerical diffusion in the simulation of STT events.

[45] Moreover, only the models with detailed resolution (i.e. LAGRANTO, FLEXTRA and FLEXPART), were able to reveal totally the input of stratospheric air over the CIM measurement site on 28–29 May 1996. This confirms, that even in a more general meaning the horizontal resolution appeared to be important for STT simulations.

[46] **Acknowledgments.** Authors thank ECWMF for providing us with their analysis; W. Fricke and H. Claude (Deutscher Wetterdienst) for Hohenpeißenberg data, and the Swiss Meteorological Institute for Payerne data. The work on the Beryllium isotopes from Jungfraujoch has been funded by the Bundesamt fuer Bildung und Wissenschaft (BBW), Bern. Filter samples from Jungfraujoch were provided by EMPA. Relative humidity data were provided by Meteo Schweiz, Kundendienst Bodendaten, Zurich. Ozone data for Jungfraujoch were provided by BUWAL (the Swiss Agency for Environment, Forest and Landscape). Finally, the diligence of the technical staff of all the stations is acknowledged and in particular U. Bonafé, F. Calzolari and F. Evangelisti for their activity at Mt. Cimone. This study was part of EU-project STACCATO (EVK2-1999-00136), funded by the European Commission under Framework Programme IV, Environment and Climate. Part of the measurement data were carried out during the EU-project VOTALP (ENV4-CT95-0025).

References

Aebischer, U., and C. Schaer, Low-level potential vorticity and cyclogenesis to the lee of the Alps, *J. Atmos. Sci.*, *55*, 186–207, 1998.

Appenzeller, C., and H. C. Davies, Structure of stratospheric intrusions into the troposphere, *Nature*, *358*, 570–572, 1992.

Appenzeller, C., H. C. Davies, and W. A. Norton, Fragmentation of stratospheric intrusions, *J. Geophys. Res.*, *101*, 1435–1456, 1996.

Austin, J. F., and M. J. Follows, The ozone record at Payerne: An assessment of the cross-tropopause flux, *Atmos. Environ.*, *25A*, 1873–1880, 1991.

Bonasoni, P., F. Evangelisti, U. Bonafé, F. Ravegnani, F. Calzolari, A. Stohl, L. Tositti, O. Tubertini, and T. Colombo, Stratospheric ozone in-

trusion episodes recorded at Mt. Cimone during VOTALP project: Case studies, *Atmos. Environ.*, *34*, 1355–1365, 2000.

Buzzi, A., G. Giovanelli, T. Nanni, and M. Tagliazucca, Study of high ozone concentrations in the troposphere associated with lee cyclogenesis during ALPEX, *Beitr. Phys. Atmos.*, *57*, 380–392, 1984.

Buzzi, A., G. Giovanelli, T. Nanni, and M. Tagliazucca, Case study of stratospheric ozone descent to the lower troposphere during ALPEX, *Beitr. Phys. Atmos.*, *58*, 399–406, 1985.

Collins, W. J., D. S. Stevenson, C. E. Johnson, and R. G. Derwent, Tropospheric ozone in a global scale three-dimensional Lagrangian model and its response to Nox emission controls, *J. Atmos. Chem.*, *26*, 223–274, 1997.

Collins, W. J., R. G. Derwent, C. E. Johnson, and D. S. Stevenson, A comparison of two scheme for the convective transport of chemical species in a Lagrangian global chemistry model, *Q. J. R. Meteorol. Soc.*, in press, 2003.

Danielsen, E. F., Stratosphere-troposphere exchange based upon radioactivity, ozone, and potential vorticity, *J. Atmos. Sci.*, *25*, 502–518, 1968.

Davies, T. D., and E. Schuepbach, Episodes of high ozone concentrations at the earth's surface resulting from transport down from the upper troposphere/lower stratosphere: A review and case studies, *Atmos. Environ.*, *28*, 53–68, 1994.

Dibb, J. E., L. D. Meeker, R. C. Finkel, J. R. Southon, M. W. Caffee, and L. A. Barrie, Estimation of stratospheric input to the Artic troposphere: ^{7}Be and ^{10}Be in aerosol at Alert, Canada, *J. Geophys. Res.*, *99*, 12,855–12,864, 1994.

Dutkiewicz, V. A., and L. Husain, Stratospheric and tropospheric components of ^{7}Be in surface air, *J. Geophys. Res.*, *90*, 5783–5788, 1985.

Eisele, H., H. E. Scheel, R. Sladkovic, and T. Trickl, High resolution Lidar measurements of stratosphere-troposphere exchange, *J. Atmos. Sci.*, *56*, 319–330, 1999.

Elbern, H., J. Kowol, R. Sladkovic, and A. Ebel, Deep stratospheric intrusions: A statistical assessment with model guided analysis, *Atmos. Environ.*, *31*, 3207–3226, 1997.

Feldmann, H., M. Memmesheimer, A. Ebel, P. Seibert, G. Wotawa, H. Kromp-Kolb, T. Trickl, and A. Prevot, Evaluation of a regional scale model for the Alpine region with data from the VOTALP Project, in *Proceeding of EUROTRAC-2 Symposium 1998*, edited by P. M. Borrell and P. Borrell, pp. 483–488, WIT Press, Southampton, 1999.

Fischer, H., N. Eigenwilling, and H. Muller, Information content of METEOSAT and Nimbus/THIR water vapor channel data: Altitude association of observed phenomena, *J. Appl. Meteorol.*, *20*, 1344–1352, 1982.

Follows, M. J., and J. F. Austin, A zonal average model of the stratospheric contributions to the tropospheric ozone budget, *J. Geophys. Res.*, *97*, 18,047–18,060, 1992.

James, P., H. E. Scheel, A. Stohl, and T. Trickl, Deep stratospheric air intrusions—Case studies and climatology. A contribution to subproject TOR2, paper presented at EUROTRAC Symposium 2002, in press, 2003.

Jeuken, A., P. Siegmund, L. Heijober, J. Feichter, and L. Bengtsson, On the potential of assimilating meteorological analyses in a global climate model for the purpose of model validation, *J. Geophys. Res.*, *101*, 16,939–16,950, 1996.

Koch, D. M., and M. E. Mann, Spatial and temporal variability of ^{7}Be surface concentration, *Tellus*, *48B*, 387–396, 1996.

Koch, D. M., D. J. Jacob, and W. C. Graustein, Vertical transport of tropospheric aerosol as indicated by ^{7}Be and ^{210}Pb in a chemical tracer model, *J. Geophys. Res.*, *101*, 18,651–18,666, 1996.

Land, C., and J. Feichter, Stratosphere-troposphere exchange in a changing climate simulated with the general circulation model MAECHAM4, *J. Geophys. Res.*, *108*(D12), doi:10.1029/2002JD002543, in press, 2003.

Li, D., and K. P. Shine, A 4-dimensional ozone climatology for UGAMP models, *UGAMP Intern. Rep. 35*, 1995.

Manzini, E., and N. A. McFarlane, The effect of varying the source spectrum of a gravity wave parameterization in a middle atmosphere general circulation model, *J. Geophys. Res.*, *103*, 31,523–31,539, 1998.

Masarik, J., and J. Beer, Simulation of particle fluxes and cosmogenic nuclide production in the Earth's atmosphere, *J. Geophys. Res.*, *104*, 12,099–12,111, 1999.

Meijer, E. W., P. F. J. van Velthoven, A. M. Thompson, L. Pfister, H. Schlager, P. Schulte, and H. Kelder, Model calculations of the impact of NO_x from air traffic, lighting, and surface emissions, compared with measurements, *J. Geophys. Res.*, *105*, 3833–3850, 2000.

Price, J. D., and G. Vaughan, Statistical studies of cut-off low systems, *Ann. Geophys.*, *10*, 96–102, 1992.

Raisbeck, G. M., F. You, M. Fruneau, J. M. Loiseaux, M. Lieuvin, and J. C. Ravel, Cosmogenic ^{10}Be/^{7}Be as a probe of atmospheric transport processes, *Geophys. Res. Lett.*, *8*, 1015–1018, 1981.

Reed, R. J., A study of a characteristic type of upper-level frontogenesis, *J. Meteorol.*, *12*, 226–237, 1955.

Reiter, R., K. Munzert, H. J. Kanter, and K. Poetzl, Cosmogenic radionuclides and ozone at a mountain station at 3.0 Km a.s.l., *Arch. Meteorol. Geophys. Bioklimatol.*, *32B*, 131–160, 1983.

Roeckner, E., K. Arpe, L. Bengtsson, M. Christoph, M. Claussen, L. Dmenil, M. Esch, M. Giorgetta, U. Schlese, and U. Schulzweida, The atmospheric general circulation model ECHAM-4: Model description and simulation of present day climate, *Rep. 218*, Max-Plank-Inst. for Meteorol., Hamburg, Germany, 1996.

Roelofs, G. J., and J. Lelieveld, Model study of influence of cross-tropopause O_3 transport on tropospheric O_3 levels, *Tellus*, *49B*, 38–55, 1997.

Scheel, H. E., R. Sladkovic, and H. J. Kanter, Ozone variations at the Zugspitze (2962 m a.s.l.) during 1996–1997, in *Proceeding of EUROTRAC-2 Symposium 98*, edited by P. M. Borrell and P. Borrell, pp. 260–263, WIT Press, Southampton, 1999.

Schuepbach, E., T. D. Davies, and A. C. Massacand, An unusual springtime ozone episode at high elevation in the Swiss Alps: Contributions both from cross-tropopause exchange and from the boundary layer, *Atmos. Environ.*, *33*, 1735–1744, 1999.

Stohl, A., and D. J. Thomson, A density correction for Lagrangian particle dispersion models, *Boundary Layer Meteorol.*, *90*, 155–167, 1999.

Stohl, A., G. Wotawa, P. Seibert, and H. Kromp-Kolb, Interpolation errors in wind field as a function of spatial and temporal resolution and their impact on different types of kinematic trajectories, *J. Appl. Meteorol.*, *34*, 2149–2165, 1995.

Stohl, A., M. Hittenberger, and G. Wotawa, Validation of the Lagrangian particle dispersion model FLEXPART against large scale tracer experiments, *Atmos. Environ.*, *32*, 4245–4246, 1998.

Stohl, A., et al., The influence of stratospheric intrusions on alpine ozone concentrations, *Atmos. Environ.*, *34*, 1323–1354, 2000.

Stohl, A., L. Haimberger, M. P. Scheele, and H. Wernli, An intercomparison of results from three trajectory models, *Meteorol. Appl.*, *8*, 127–135, 2001.

Tafferner, A., Lee cyclogenesis resulting from the combined outbreak of cold air and potential vorticity against the Alps, *Meteorol. Atmos. Phys.*, *43*, 31–47, 1990.

Trickl, T., Intercontinental transport and its influence on the ozone concentration in the free troposphere over central Europe, *J. Geophys. Res.*, *108*(D12), doi:10.1029/2002JD002735 in press, 2003.

Vaughan, G., and J. D. Price, Ozone transport into the troposphere in a cut-off low event, in *Ozone in the Atmosphere*, edited by R. D. Bojkov and P. Fabian, pp. 415–416, A. Deepak, Hampton, Va., 1989.

Wernli, H., and H. C. Davies, A Lagrangian based analysis of extratropical cyclones, 1, The method and some applications, *Q. J. R. Meteorol. Soc.*, *123*, 467–489, 1997.

Wirth, V., C. Appenzeller, and M. Juckes, Signatures of induced vertical air motion accompanying quasi-horizontal roll-up of stratospheric intrusions, *Mon. Weather Rev.*, *125*, 2504–2519, 1997.

Zanis, P., E. Schuenpbach, H. W. Gaeggeler, S. Huebener, and L. Tobler, Factors controlling Beryllium-7 at Jungfraujoch in Switzerland, *Tellus*, *51*, 789–805, 1999.

P. Bonasoni and P. Cristofanelli, National Research Council, Institute of Atmosphere Sciences and Climate (ISAC), Bologna, Italy. (P.Cristofanelli@isac.cnr.it)

W. Collins, Climate Research, Met Office (MetO), Bracknell, UK.

J. Feichter and C. Land, Max-Planck Institute for Meteorology (MPI), Hamburg, Germany.

C. Forster, P. James, and A. Stohl, Department of Ecology, Technical University of Munich (TUM), Freising-Weihenstephan, Germany.

A. Kentarchos and G. J. Roelofs, Institute for Marine and Atmospheric Research (IMAU), University of Utrecht, Utrecht, Netherlands.

P. W. Kubik, Paul Scherrer Institute, c/o ETH Hoenggerberg, Zurich, Switzerland.

J. Meloen and P. Siegmund, Division of Atmospheric Composition, Royal Netherlands Meteorological Institute (KNMI), de Bilt, Netherlands.

C. Schnabel, Department of Chemistry and Biochemistry, University of Berne, Berne, Switzerland.

M. Sprenger, Institute for Atmospheric and Climate Sciences, Swiss Federal Institute of Technology Zurich (ETHZ), Zurich, Switzerland.

L. Tobler, Paul Scherrer Institute, Villigen, Switzerland.

L. Tositti, Environmental Radiochemistry Laboratory, Bologna University, Bologna, Italy.

T. Trickl, Institut fuer Meteorologie und Klimaforschung (IMK-IFU), Bereich Atmosphaerische Umweltforschung, Forschungzentrum Karlsruhe, Garmisch-Partenkirchen, Germany.

P. Zanis, Laboratory of Atmospheric Physics, Aristotle University of Thessaloniki, Greece.